國立臺灣大學公共衛生學院環境衛生研究所

碩士論文

Graduate Institute of Environmental Health

College of Public Health

National Taiwan University

Master Thesis

慢濾池降低水中亞硝基二甲胺濃度之研究

N-Nitrosodimethylamine Reduction by Slow Sand

Filtration during Drinking Water Treatment

張景瑜

Chang, Ching-Yu

指導教授：王根樹 博士

童心欣 博士

Advisors: Wang, Gen-Shuh, Ph.D.

Tung, Hsin-Hsin, Ph.D.

中華民國 99 年 10 月

October, 2010

中文摘要

　　許多研究證實淨水廠或廢水處理廠的加氯消毒會生成包括亞硝基二甲胺 (*N*-Nitrosodimethylamine；NDMA)等不同類別的消毒副產物。在動物實驗上，亞硝基二甲胺具有致基因變異的特性，因此美國環保署 (USEPA) 將其分類為可能的人類致癌物質 (Group B2)，且其致癌性遠遠高於傳統消毒副產物，如三鹵甲烷 (Trichloromethanes；THMs) 與含鹵乙酸 (Haloacetic acids；HAAs)。為了確保公眾健康，避免飲用水中出現亞硝基二甲胺為十分重要的議題。過去研究顯示紫外光可以有效地光解亞硝基二甲胺，然而其所需的成本相當高，且水中可能進一步生成亞硝基二甲胺的前驅物質。近來陸續有研究針對亞硝基二甲胺的生物降解進行探討，包括培養環境微生物與實場調查研究。然而，嘗試在實場樣品中純化出可以降解亞硝基二甲胺的微生物時卻總是未能成功，因此無法進一步了解這些微生物分解亞硝基二甲胺的機制與特性。

　　本研究針對實場能減少水中亞硝基二甲胺的微生物進行物種鑑定，瞭解會影響亞硝基二甲胺進行生物轉換的環境因素，以及調查這些微生物在實場的分佈比例情形。首先，以塗抹與劃碟法於淨水場慢濾單元中純化出不同的微生物，再進行生物處理亞硝基二甲胺的測試。接著針對具有去除液態基質中亞硝基二甲胺能力的微生物進行動力學實驗，並且改變不同環境因子檢視其對生物處理效率的影響；包括亞硝基二甲胺起始濃度、溫度、實場進流水中基質、以及混菌狀態的影響等等。同時於實驗室建立模擬濾砂管柱系統，以實場慢濾池進流水添加亞硝基二甲胺進行微生物馴養與處理效率的探討。最後利用末端限制片段長度多型性 (Terminal restriction fragment length polymorphism；T-RFLP) 分析冬季與夏季時，減少水中亞硝基二甲胺濃度的微生物實場分佈，同時也探討其於模擬管柱的空間分布情形。

　　本研究於慢濾池濾砂生物膜中純化出具有降低水中亞硝基二甲胺能力的微生

物，鑑定結果為甲基桿菌屬（*Methylobacterium* sp.) 的物種。此菌種並非以亞硝基二甲胺作為生長營養物質，而是經由共代謝的形式將其分解，測試後發現可催化共代謝的物質為一複合培養基，R2A。動力學結果顯示，在 25℃和 15℃時，亞硝基二甲胺起始濃度越高，反應速率常數與十小時去除百分比越低，如起始濃度為 600 μg/L 的十小時去除百分比相較於起始濃度 50 μg/L 時減少至少 70%，表示去除效率減低。然而在 35℃時，亞硝基二甲胺起始濃度改變對去除效率並沒有顯著影響，低濃度的十小時去除百分比只比高濃度高出 7%。比較相同起始濃度下，25℃去除效率較 15℃好，但是在 35℃時發現溫度過高也會影響生物處理效率。比較三個環境溫度的結果，反應最高速率(V_{max})在 25℃ 的環境下最高 (30 μg/L/hour)，因此表示常溫反應的生物處理效率最好。此外，以 100%無菌慢濾池進流水作為批次反應基質時，去除百分比減少為 5.4%，顯示慢濾池水中有機或無機物質組成可能會影響生物處理的效率。而在模擬的混菌環境下亞硝基二甲胺的去除百分比和純菌結果相似，但是甲基桿菌菌種在混菌環境下的生長速度相對緩慢。

根據末端限制片段長度多型性分析（T-RFLP）結果，冬季濾砂中甲基桿菌菌種的比例為夏季的兩倍。雖然模擬濾砂管柱系統並無顯著去除水中亞硝基二甲胺，但是在第二層管柱濾砂中有偵測到此株甲基桿菌菌種，推測也許模擬的條件仍與實場條件差異甚大，如亞硝基二甲胺與溶解性有機碳(NPDOC)的比例差異，因而影響其生物處理亞硝基二甲胺的能力。

研究結果顯示，淨水場中的慢濾單元存在有甲基桿菌菌種，因此具有去除水中亞硝基二甲胺的潛能。然而，實際操作時水中有機物質、混菌環境、以及環境溫度改變的影響，都是必需要考量的因素。

關鍵詞：亞硝基二甲胺、消毒副產物、生物降解、慢砂濾、末端限制片段長型性、甲基桿菌屬、共代謝

Abstract

N-Nitrosodimethylamine (NDMA) was recently found as one of the emerging disinfection by-products (DBPs) in the wastewater and drinking water treatments. The toxicity of NDMA, which has been classified by USEPA as Group B2 of probable human carcinogen, was much higher than that of conventional DBPs such as THMs and HAAs. Thus, the control of NDMA in drinking water is an important issue for public health protection. Previous studies showed that NDMA can be destructed effectively by UV irradiation; however, it requires high UV dosage and NDMA precursors are likely to be formed again after UV treatment. Recently, microbial degradation of NDMA was studied extensively in laboratory and field investigations. However, isolation of NDMA-degrading bacteria from the field was not successful. Hence, the information regarding to the NDMA biotransformation mechanisms in the field was limited.

The objectives of this study were to identify the organisms responsible for the bio-reduction of NDMA, to provide information concerning environmental factors affecting the efficiency of NDMA biotransformation, and to investigate the distribution of NDMA-reducing bacteria in the field.

First, the candidates of NDMA-reducing bacteria were isolated from the biofilm attached on the slow sand filter in a water treatment plant by traditional plating methods. Followed by NDMA bio-reduction capability tests, kinetic experiments were conducted

to demonstrate the roles of initial NDMA concentrations and environmental factors on NDMA removal. Third, a laboratory simulated sand column system was installed to establish a natural distribution of microbes along different depths of the column through continuous acclimation. Finally, the distribution of NDMA-reducing bacteria in the slow sand filter obtained in different seasons and which from simulated sand column was analyzed by terminal restriction fragment length polymorphism (T-RFLP).

The *Methylobacterium* sp. was isolated from the slow sand filter, and the ability of NDMA bio-reduction was observed after growth on a low nutrient medium, R2A. The bacterial isolate was unable to grow in the presence of NDMA, but it performed NDMA biotransformation through possible cometabolism when incubated with R2A medium. In the kinetic experiments, first-order and second-order reaction equations were used to fit the kinetic data from the reduction curve. The results demonstrated that 1st and 2nd order kinetic reaction rate constants ($hour^{-1}$) and percent removal after 10 hours of contact time increased as the initial concentration decreased at 25℃ and 15℃, but no significant difference was found at 35℃. For the same NDMA initial concentration, the rate constant and extent of NDMA removal were higher at 25℃ than 15℃, however, biotransformation of NDMA seemed unfavorable to the bacterial isolate for a higher temperature at 35℃. Also, the enzyme's maximum rate, V_{max}, was the highest at 25℃. It was suggested that the optimal temperature for NDMA biotransformation was

approximately at room temperature for the isolated *Methylobacterium* sp.. Different

proportions of sterile influents from slow sand filter were spiked into the reaction matrix,

and the percentage of NDMA removal in 100% of field scale influent water was only

5.4%, revealing that the compositions of organic or inorganic compounds in the filter

influent might affect the efficiency of NDMA bio-reduction in the slow sand filter. In

addition, mixed bacteria might have no direct influence on NDMA bio-reduction, but it

could affect the growth of the *Methylobacterium* sp..

T-RFLP showed that NDMA-reducing bacteria like *Methylobacterium* sp. was

detected in the slow sand filter, and its relative proportion as total community were

two-fold increased in the winter than in the summer.

The laboratory simulated sand column fed with influents was spiked with 100 μg/L

NDMA, but no significant NDMA reduction was observed during the study. However, a

natural spatial distribution of microorganisms was formed, and the *Methylobacterium* sp.

isolate was detected in the upper-middle layer of the laboratory column by T-RFLP

analysis. It is possible that growth conditions for laboratory column were different than

in the field.

Contents

List of Figures

List of Tables

Chapter I   Introduction

1.1   Background

N-Nitrosodimethylamine (NDMA) has been classified by U.S. EPA as Group B2, probable human carcinogen [1, 2]. In addition to their widespread occurrence in food and consumer products [3, 4], NDMA becomes an environmental concern due to its presence in rocket fuel-contaminated groundwater [5] and as an emerging disinfection byproduct in wastewater and drinking water treated with chloramines and/or other disinfectants [6-8]. Because of its high water solubility, NDMA was poorly removed from water [1, 3]. Currently, UV irradiation was considered as the most efficient treatment method for the control of NDMA in drinking water, but it requires much higher UV dosage than disinfection needs and may further increase NDMA precursors formation [5, 9].

Many studies demonstrated that NDMA was biodegradable under aerobic or anaerobic conditions [10]. Several studies also found NDMA-degrading bacteria in the groundwater remediation systems [11, 12]. NDMA biodegradation in the environments has received many interests recently since it is a cost-effective method [13]. However, isolation of the NDMA-degrading bacteria from the field was not successful [10, 14]. There was limited information available regarding to the organisms responsible for the

NDMA biodegradation in the field.

Recently, a field-scale study conducted in the drinking water treatment plant in Kinmen has shown that NDMA concentration was reduced by as much as 70% in the slow sand filtration unit [15]. Since slow sand filtration might be considered as biofilters, where microbial biomass accumulated on the sand surface (schmutzdecke layer) [16], it is possible that NDMA could be removed through biofiltration treatment process.

In this study, microbial biomass from slow sand filter was used for biodegradation experiments. Instead of enrichment cultivation by amending high concentration of NDMA, we attempt to use a low-nutrient medium, R2A, to isolate oligotrophic bacteria from slow sand filtration unit. After isolation and purification process, the bacteria isolates were then tested for their NDMA bio-reduction capability, and kinetic experiments were carried out in order to evaluate the factors affecting rates of NDMA biotransformation. A simulated sand column fed with field influent of slow sand filter was constructed to acclimate the NDMA-degrading bacteria and to establish spatial microbial distribution in the column. Seasonal variations and spatial distribution of NDMA-reducing bacteria were then investigated via T-RFLP method using field sand samples and the sand collected from the simulated column, respectively. Furthermore, community diversity was compared from the fingerprint patterns as well.

1.2　　**Objectives of this study**

The objectives of this study are as follows,

1.2.1　To isolate and characterize the microorganisms responsible for the bio-reduction

of NDMA in slow sand filters.

1.2.2　To provide information regarding environmental factors affecting the efficiency

of NDMA biotransformation.

1.2.3　To investigate the seasonal variations and spatial distribution of

NDMA-reducing bacteria in the slow sand filter.

Chapter II   Literature Review

2.1   Molecular structure and properties of *N*-nitrosodimethylamine

N-Nitrosodimethylamine (Figure 2.1) is also named dimethylnitrosoamine, *N*-methyl-*N*-nitrosomethanamine, *N*-nitroso-*N,N*-dimethylamine, and abbreviated as NDMA, DMN, or DMNA [2, 3]. NDMA is an oily, yellow liquid which has no distinct odor [1]. It is soluble in water and many organic solvents, such as alcohols and ethers, due to the presence of the polar functional groups [1, 5, 17]. The estimated Henry's Law constant at 20℃ is 2.6×10^{-4} atm M^{-1}, so that NDMA as a semi-volatile organic compound will be retained in water rather than evaporate to atmosphere. Table 2.1 summarizes the physical and chemical properties of NDMA [3, 18, 19].
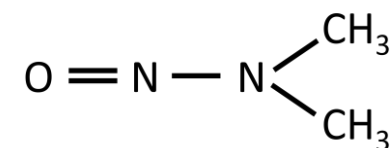
Figure 2. 1   Molecular structure of *N*-nitrosodimethylamine (NDMA)

Table 2. 1   Physical and chemical properties of *N*-nitrosodimethylamine (NDMA)

Property	Value
Chemical formula	$C_2H_6N_2O$
Molecular weight	74.08 g/mol
CAS number	62-75-9
Melting point	50℃
Boiling point	154℃
Log octanol-water partition coefficient (log K_{ow})	-0.57
Specific gravity	1.0059 g/ml
Vapor pressure at 20℃	2.7 mmHg

2.2   Environmental occurrence and human exposure

2.2.1   Exposure sources and occurrence in the drinking water systems

Since 1960s, NDMA was first found in the diet; hence, many studies have focused

on the health effects of nitrosamines [5]. NDMA was formed from the constituents in

food, mainly dimethylamine (DMA) and trimethylamine (TMA). During food

processing, nitrite and/or nitrate additions, food dried by nitrogen oxides containing

combustion gases will cause many nitrosating agents introduced into the foodstuffs.

Therefore, NDMA is detectable in various foods including meat, cured meat products,

smoking fish, milk, and pickled vegetables [1, 3, 4]. NDMA has also been detected in

many consumer products, such as cosmetics, rubber products, tobacco smokes, and

personal care products [3]. Recently, the Food and Drug Administration (FDA) has set

an action level of 10 ppb for individual nitrosamines in rubber baby bottle nipples [20].

NDMA is also occurred in the water environments and has caused public concerns

recently. At first, the effluents of rocket engine manufactory in Sacramento County, CA,

which used the rocket fuel containing unsymmetrically dimethylhydrazine (UDMH),

had contaminated nearby drinking water wells. After the oxidation of UDMH, the

groundwater NDMA concentrations were detected at levels as high as 400,000 ng/L on

site and 20,000 ng/L off site [5]. In 1989, a survey of drinking water plants conducted in

Ontario, Canada, demonstrated that most of the treated water containing less than 5 ng/L

of NDMA, but some of them may exceed 9 ng/L [4]. . So far, there were no regulations

established for NDMA in drinking water in US, but several agencies have established

their own guidelines. For instance, The Ontario Ministry of the Environment and

Energy had set an Interim Maximum Acceptable Concentration for NDMA at 9 ng/L [5].

Another study conducted in California [6] had reported that NDMA was detected as a

disinfection by-product in the treated water from several water utilities. Based on their

studies, degree of chloramination, types and dosages of cationic polymers and contact

times were the major factors affecting the levels of NDMA concentrations in the treated

water. Besides, the investigation of NDMA concentrations from surface water treatment

plants in California has showed that ozone and/or chlorine disinfection will also

produce NDMA in ng/L level. After the surveys in water utilities and development of

NDMA analysis at low-level concentration, California Department of Health Service

(CDHS) set a notification level of 10 ng/L for NDMA in drinking water. Recently,

treated wastewaters were intentionally or unintentionally entering the sources of

drinking water treatment plant, so the presence of NDMA has became more important.

In 2000, NDMA above 20 ng/L was detected in two drinking water wells, which

received the treated effluent water from Orange County Water District's (OCWD) Water

Factory 21 [21]. NDMA occurrences in wastewaters had been reported extensively and

the level of NDMA concentrations were much higher than that of treated drinking water

[5, 22], in some cases higher than 100 ng/L [17].

2.2.2   NDMA precursors and its formation mechanisms

Since NDMA was detected in the treated drinking water and wastewater, the

mechanisms of NDMA formation were proposed in some studies. Two major pathways

of NDMA formation were proposed, including nitrosation and oxidation of UDMH [5].

Formation of NDMA in foods and consumer products as mentioned in previous

section was occurred through nitrosation mechanisms [23]. Nitrite and/or

nitrogen-containing species, such as NO_x or nitroso radicals, were involved in this

reaction. Nitrosation was first occurred at acidic condition for converting nitrite to

nitrous acid (HNO_2, pK_a of HNO_2 =3.37), and subsequently to yield the nitrosating

species, e.g. nitrous cation (NO^+), nitrous anhydride (N_2O_3), or nitrosyl halide (NO_X).

These nitrosating species then reacted with an amine from the constituents of food or

consumer products, mainly dimethylamine (DMA, pK_a of protonated DMA =10.7), to

form the NDMA. The overall reaction was carried out rapidly at pH 3.4, but several

studies have demonstrated that NDMA was observed even at neutral or basic pH under

natural environmental conditions [24, 25].

The second NDMA formation pathway was the oxidation of UDMH, which was

the by-product of industrial processes or ingredients of rocket fuels and reported as an

contaminant in groundwater. In contrast to nitrosation, the process was carried out most

rapidly at neutral and high pH conditions [26]. As the surveys and researches conducted

in water utilities in California, NDMA was detected in treated water [6]. Recently, many

studies have focused on the NDMA formation during chlorination, and most of the

results reported that NDMA was formed from the reaction of monochloramine and

dimethylamine [8, 27], even though several studies had assumed that nitrosation

pathway was also involved in the NDMA formation [28, 29]. A two-step mechanisms

were proposed by Mitch and Sedlak [8] and Choi and Valentine [27]. In the two-step

mechanism, UDMH was the reaction product of monochloramine and DMA, and the

rate of UDMH formation was increased with pH but the reaction was also observed at

neutral pH. This was the rate-limiting step, and the UDMH intermediate was then

quickly oxidized to NDMA. The yield of NDMA was maximized when the concentration of monochloramine was fixed with varied DMA, revealing the important role of monochloramine on NDMA formation. In these studies, they also conducted the experiments using sodium hypochlorite as the disinfectant to react with DMA in water, and the results revealed that NDMA was formed when the sodium hypochlorite was used alone. Bromide ion in the raw water was another important factor for NDMA formation. In the presence of ammonia, bromide was reacted with sodium hypochlorite to produce bromamine, which was chemically similar to the structure of chloramines [30]. Therefore, the existence of bromide in raw water of water treatment plants, especially on the off-shore island of Taiwan, may have a catalytic effect on NDMA formation.

Except for the chlorine and chloramination, other water treatment processes may also lead to different levels of NDMA formation. Zhao *et al.* [31] investigated the effects of different treatments in various surface waters on NDMA formation, including oxidation with chlorine, chloramines, ozone, UV, chlorine dioxide, advanced oxidation process (AOP), and their combinations. According to their results, NDMA was significantly formed after chlorine, chloramine, and ozone treatments; in contrast, UV was effective to remove NDMA under low turbidity and color. However, following UV, ozone, and AOP treatments, NDMA was increased by subsequent addition of chlorines.

This suggested that UV, ozone, AOP treatments may further cause NDMA precursors formation.

Both of the formation pathways mentioned earlier have showed that DMA was an important organic precursor for NDMA formation, but other nitrogen-containing organic compounds, especially with dimethyl functional groups, have been shown as the potential NDMA precursors [5, 32, 33].

2.2.3 Toxicology and risk assessment

NDMA was classified by U.S. EPAas Group B2 probable human carcinogen due to the evidence for its carcinogenicity in animal studies [2]. However there were only limited information available for human exposure health effects due to the many confounding factors. However, animal studies had demonstrated that NDMA may produces liver tumors in BD rats and in female Porton rats when administrated in drinking water and diet, respectively [34, 35]. Because the primary exposure pathway of NDMA was the oral ingestion [19], U.S. EPA had established a cleanup level of 0.7 ng/L in drinking water based on the risk assessment for lifetime excess cancer risk of 10^{-6} from oral exposure [36].

2.3 Physical and chemical methods for removal of NDMA

As a semi-volatile compound, NDMA is hardly eliminated from water by air stripping [5]. Many porous materials were used to remove organic compounds in water,

but they were not suitable for NDMA removal due to its small and polar characteristics [1, 17]. Field evidence have shown that adsorption onto soil and granular activated carbon (GAC) was insignificant for NDMA [11].

Reverse osmosis (RO) filtration was efficient to reject many organic compounds, however, NDMA could pass through the porous membrane since the molecular weight of NDMA was smaller than the reported molecular weight cut-offs (MWCO) of membranes [37]. Steinle-Darling *et al*. [38] demonstrated that membrane types, coating, fouling, chemical properties and water parameters had large impacts on NDMA removal. The rejection of NDMA in deionized water was approximately 56-70% by reverse osmosis. But within the wastewater recycling plants, NDMA was removed at about 50% efficiency [5].

Ozone is a strong oxidant, which can react directly with organic compounds or decompose to hydroxyl radical which possessed stronger oxidation ability than molecular ozone [39]. Lee *et al.* [40] investigated the efficiency of NDMA oxidation by conventional ozonation and advanced oxidation process (AOP) using ozone/hydrogen peroxide (O_3/H_2O_2) in lake waters. Their results demonstrated that less than 25% of NDMA was removed via conventional ozonation, and higher ozone dosage (>160 μM) was needed for AOP treatment to achieve 50-75 % of NDMA oxidation. Also, bromate ion (BrO_3^-), which was a potent carcinogen and regulated in drinking waters at many

countries, was formed during ozonation in bromide-containing waters [41, 42].

Therefore, ozonation was not a good technique for treatment of NDMA in drinking

water.

Many literatures have provided a lot of treatment methods for NDMA in drinking

water and made some comparisons between the various techniques, but currently, the

most widely used method was photolysis with ultraviolet (UV) radiation [5]. The

absorption spectra of NDMA showed that NDMA absorbs the UV light with

wavelengths between 225 and 250 nm, and the weaker absorption wavelength ranges

were between 300 and 350 nm. The photolysis reactions were conducted at pH 7 and pH

3, and the TOC was decreased by 13% at pH 7 but no significant change was obtained

at pH 3. The NDMA photolysis produced dimethylamine (DMA), nitrite and nitrate as

the major degradation products, and other minor products were formaldehyde, formic

acid, and methylamine (MA) [9]. Lee *et al*. [43] proposed the dual pathways of NDMA

photolysis to MA versus DMA, and the two pathways were strongly dependent on the

initial NDMA concentration and the pH of the solutions. Even though the UV treatment

was highly efficient for NDMA removal, the UV dosage required for NDMA

degradation was approximately 10 times higher than the UV dosage needed for

disinfection alone. Thus, for economic considerations, sunlight photolysis which

occurred with sunlight between 300 and 350 nm was an alternative method for NDMA

removal in the water treatment plant [5]. Nevertheless, there are still many limited factors affecting the efficiency of NDMA photolysis, either by sunlight or UV reactors, such as the interference of organic matters in water and the depth of water basins [44, 45].

Advanced oxidation processes (AOP) were widely used for NDMA removal in the wastewater treatments. An investigation for the efficiency of NDMA removal by AOP was conducted by Plumlee *et al*. (2008) using the advanced treatments at the Interim Water Purification Facility in California [46]. In this study, the secondary effluent from an activated sludge treatment unit was treated with microfiltration (MF), reverse osmosis (RO), and UV/H_2O_2 process, sequentially. As expected, the results showed that MF was not able to reduce NDMA effectively, and it might form NDMA during chloramination or chlorination to prevent MF membrane fouling. Removal of NDMA by RO and UV/H_2O_2 process were ranged from 24 to 56% and 43 to 66%, respectively. The overall of NDMA removal was 67±7% for the secondary effluent.

2.4   Biodegradation of NDMA

Biodegradation, which is also a natural attenuation process to remove NDMA in water, had recently received great interests because of its cost-effectiveness and less harmful to the environments [13].

2.4.1 Environmental evidence

Biodegradation of NDMA have been observed in soil and aqueous environments [10, 14]. An intercept-and-treat system at the Rocket Mountain Arsenal (RMA) was established to remove toxic contaminants, including NDMA, in a groundwater plume. The results showed that the major attenuation mechanism was mineralization of NDMA occurring in soils under both aerobic and anaerobic conditions [11]. Another study also investigated the biodegradation of NDMA in soil from a water reclamation facility in California. It was observed that more than 54% of NDMA was transformed to CO_2 or CO_2 and CH_4 under oxic or anoxic conditions, respectively [12]. Furthermore, Zhou *et al*. [47] developed a fate and transport model of NDMA degradation using surface water and groundwater monitoring data to estimated NDMA degradation in groundwater recharged with recycled waters. The results demonstrated that approximately 80% of the recharged mass was biodegraded in the subsystem. In addition, many studies have demonstrated that NDMA concentration was significantly lower in the secondary effluents of activated sludge or anaerobic digested systems than primary effluent in wastewater treatment plants [22, 48, 49]. However, the microorganisms responsible for NDMA degradation in nature were still not clear [10, 14].

2.4.2 Laboratory incubation studies and cometabolism effects

In a laboratory study [10], a simulated activated carbon trickling filter was

constructed and acted as a growth matrix for NDMA-degrading bacteria. The results

showed that the cell growth was very sparse on the filter, but NDMA was significantly

mineralized after a long period incubation. This phenomenon was further elucidated by

several studies regarding mechanisms of NDMA biodegradation, which were conducted

by axenic bacterial cultures instead of mixed consortia from the field.

In eukaryotes, it has been proven that cytochrome P-450 was involved in the

metabolic oxidation of NDMA [50]. Bacterial monooxygenases were functionally

similar to the eukaryotic cytochrome P-450 enzymes, and many researches have

indicated that bacterial oxygenases exhibit its ability to oxidize xenobiotics [51, 52].

Sharp *et al*. [53] demonstrated that induction of monooxygenase enzymes which

appeared in a variety of environmentally isolated bacteria cultures can cause NDMA

degradation. However, not all of the monooxygenase enzymes could oxidize NDMA;

for example, particulate methane monooxygenase-expressing *Methylosinus*

trichosporium OB3b, toluene 2-monooxygenase-expressing *Burkholderia cepacia* G4,

and toluene side chain monooxygenase-expressing *Pseudomonas putida* mt-2 were not

observed to be able to degrade NDMA. In addition, NDMA degradation by various

monooxygenase bacteria was shown to be a cometabolic process [54], and the bacterial

cultures were not able to grow with NDMA as the sole carbon and energy source [53, 55,

56]. However, a recent study found that propanotroph *Rhodococcus ruber* ENV425 was

observed to utilize NDMA as nitrogen sources when growing on propane [56].

Two distinct metabolic pathways of NDMA biotransformation were proposed for *Pseudomonas memdocina* KR1 and *Rhodococcus ruber* ENV425, respectively [55, 56]. In *P. memdocina* KR1, NDMA was first oxidized by monooxygenase to form *N*-nitrodimethylamine (NTDMA) as an intermediate, and metabolized further to *N*-nitromethylamine as a terminal product with 94% recovery and a small amount of formaldehyde. In contrast, *R. ruber* ENV425 used a denitrosation pathway to perform NDMA degradation, which was commonly observed in mammals [57, 58]. Instead of producing NTDMA, a hydrogen atom from a methyl group of NDMA was first abstracted, and then *N*-methylformadimine and nitric oxide were formed through denitrosation. Methylamine (MA), carbon dioxide (~ 60%) and nitrate were the major degradation products, and other intermediates including nitrite, formate, formaldehyde and DMA were present at relatively small quantities. Although NDMA precursor, DMA, was detected during NDMA degradation, it was not able to accumulate because it was easily metabolized by microorganisms [59].

2.4.3 Factors affecting the NDMA biodegradation efficiency

The rates of NDMA biodegradation were highly variable in the environmental matrixes [60, 61]. Several studies have discussed some factors affecting the NDMA biodegradation efficiency, which include NDMA initial concentrations, organic matters,

temperatures, degree of adaptation of the microorganisms, soil moisture contents, and so on. Kaplan and Kaplan [10] had demonstrated that rate constants (per day) were increased with decreasing NDMA initial concentrations in both soil and aqueous systems, and rates of NDMA mineralization were reduced in aqueous system when supplemented organic matters were amended. Nevertheless, sufficient amount of biodegradable organic carbon (BDOC) was needed for NDMA degradation during its cometabolic process [62]. Another study also indicated that NDMA degradation in soils was affected by reaction temperatures, which NDMA degradation was slower at 10℃ than that at room temperature [63]. NDMA degradation was almost inhibited in dry soil, but no significant differences (between 47.7 and 57% mineralization) were found among 25, 50, 75, and 100% soil moisture levels [10]. Results conducted under conditions simulating groundwater recharge operations suggested that long period of cultivations were required to develop the adapted biocommunity for NDMA removal [61, 62].

2.5   Terminal restriction fragment length polymorphism (T-RFLP)

There were many methods available to study the characteristics of microbial communities for environmental samples, including culture-dependent and culture-independent methods [64]. Terminal restriction fragment length polymorphism (T-RFLP) was one of the culture-independent methods, which is widely used to explore

the microbial diversities in various environments, like soil, biofilms, water, marine, sediments, and feces [65-68]. Compared to other methods, such as DGGE and TGGE, TRFLP requires less labor work relatively [69].

T-RFLP involved segregating individual fragment based on the sequences difference of a specific gene. Take the 16S rRNA gene as an example. Initially, a fluorescently labeled oligonucleotide primer was used to amplify a region of 16S rRNA gene from total extracted nucleic acids in the community by polymerase chain reaction (PCR). Followed by a restriction enzyme digestion of the amplicons, the fluorescence carried terminal restriction fragments (T-RFs) were separated by a capillary electrophoresis and then detected by a fluorescence detector [70]. The electropherograms showed the sizes and fluorescence intensities of T-RFs and each peak denoted an operational taxonomic unit (OTU), which is considered as a phylogenetic classification [68, 71]. The method could distinguish nucleotide fragment length difference to as small as 1 single base pair. Based on the fingerprints, the diversity and structure of the microbial community could be represented clearly.

T-RFLP had been reported to be able to detect very minor components of the whole microbial community, as low as 0.1% [71], revealing the sensitive characteristics. Also, highly reproducible capability was proved, and therefore T-RFLP fingerprints were comparable among different microbial communities [72]. There were many studies

exploring the effects of environmental transitions on the structure and composition of microbial communities by T-RFLP analysis, such as spatial variation [73, 74] and temporal dynamics [75].

Although T-RFLP was a valuable method for comparing the relationships between complex communities, it could not provide information concerning the phylotypes of T-RFs. Recently, several web-based resources were established to provide ribosome related database and data analysis performed by T-RFLP analysis [76, 77]. T-RFLP analysis program (TAP) T-RFLP (http://rdp8.cme.msu.edu/html/TAP-trflp.html) from Ribosomal Database Project (RDP) and MiCA (http://mica.ibest.uidaho.edu/) at the University of Idaho were two of the most popular resources. Fragments obtained by T-RFLP analysis from unknown community could be compared by manually scanning to find the matched fragment size of known species in the database. In addition, based on the inputs of PCR primers and restriction enzymes, predictions of T-RFs from specific bacterial sequences were accomplished. These web-based resources for T-RFLP analysis were still updating to extend the scope for more species. Liu *et al.* (1997) utilized RDP database to simulate distribution of T-RF size of 1102 complete bacterial sequences to select proper PCR primers and enzymes, which gave the largest numbers of T-RFs [70]. In their results, all bacterial strains in a model bacterial community could be distinguished and consistent with the simulated predictions by T-RFLP.

Chapter III   Materials and Methods

3.1   Field sampling

A water treatment plant (WTP) in Kinmen was selected as the study sites. In this WTP, raw water was treated with following processes - aeration, pre-chlorination, coagulation/flocculation, floatation, rapid filtration, slow sand filtration and post-chlorination. Sodium hypochlorite was used as the disinfectant during chlorination. Two field samplings were conducted to collect water and sand samples from the slow sand filtration unit of this treatment plant on 1st May 2009 and 28 November 2009, respectively. Water samples were collected from the influent of slow sand filter unit and stored at 4℃. The sand samples were collected from the top portion of the filter, which has been operated for more than three months. Composite sand samples with microorganisms were sampled from various sites of the sand filter and separated into two sterile tubes, one was stored at 4℃ for cultivation, and the other was stored at -20℃ for genetic analysis.

3.2   Isolation and identification of bacterial isolates on the biofilm of slow sand filter

3.2.1   Field sand samples pretreatment and pure bacterial cultures isolation

Fifteen grams of wet sand samples taken from the WTP in Kinmen were added to 0.22 μm filtered sterile influent of slow sand filter. The sample was first vortexed for 10

seconds and inverted the tubes vigorously for 5 times, and further sonicated for 2 minutes. This procedure was repeated for 5 times to detach the microorganisms on the sand surface. Subsequently, the sample was settled for 10 minutes and the supernatant was transferred into a sterile 50 ml centrifuge tube. After serial dilutions of the supernatant with sterilized influent, 0.2 ml of diluted suspensions was spread on the R2A agar plate (Difco[TM], USA) supplemented with 0.5 mg/L NDMA according to standard microbial techniques and incubated at 25 ℃ for 7 days. Individual colonies were picked and purified by streaking plate method.

3.2.2   Growth curve and bacterial isolate glycerol stocks preparation

The pure bacterial isolates were inoculated with R2A medium (Table 3. 1) in sterilized serum bottles separately and incubated at 25℃ with shaking at 150 rpm. Growth of the pure culture was determined every day by the optical density measurement at 600 nm (OD_{600}) using a spectrophotometer (UV-160A, Shimadzu corporation, Japan).

Bacterial glycerol stock was prepared according to the procedures described on The Condensed Protocols from Molecular Cloning [78] with slight modifications. Autoclaved sterile 50% glycerol in distilled water was first prepared for the pure culture strains stocks. A single colony of the isolated strain on the R2A agar plate was

transferred into 140 ml of fresh R2A medium and incubated at 25℃ until the early

exponential phase of growth. Next, 60 ml of sterile 50% glycerol was added to the pure

culture suspension to the final concentration of 15% glycerol and then followed by 10

minutes incubation at 25℃ while shaking at 130 rpm. A total volume of 200 ml

glycerol-culture mixture was separated into 200 tubes of sterile 1.5 ml eppendorf and

stored at -80℃ immediately.

Table 3. 1   R2A medium components

Component	Concentration (g/L)
Yeast extract	0.5
Bacto[TM] Proteose peptone No.3	0.5
Casamino acid	0.5
Dextrose	0.5
Soluble starch	0.5
Sodium pyruvate	0.3
Dipotassium phosphate	0.3
Magnesium sulfate (7 hydrate)	0.102

3.2.3 Bacterial identification by polymerase chain reaction (PCR) and nucleotide Basic Local Alignment Search Tool (BLAST)

Sequences analysis of 16S rRNA gene was conducted for the bacterial isolates. Table 3. 2 lists primers used in this study. In this section, primer pairs 8F and 1512R were used to amplify the almost full length of 16S rRNA gene. A small portion of single colony of bacterial isolate was transferred to a PCR tube by sterilized toothpick and 50 µl of reaction mixtures (Table 3. 3) were added. The PCR reaction temperature programs were as follows: initial denaturation at 94℃ for 5 minutes, followed by 30 cycles including denaturation at 94℃ for 1 minute, annealing at 58℃ for 45 seconds, extension at 72℃ for 1.5 minutes, subsequent with 10 minutes of final extension reaction at 72℃. The amplified DNA was confirmed by 1.5% agarose gel electrophoresis and the nucleotide sequences were determined by automatic DNA sequencing (Genomics BioSci & Tech, Inc., Taiwan).

Phylogenetic analysis was carried out using the resource of nucleotide Basic Local Alignment Search Tool (BLAST) in the GenBank database of National Center for Biotechnology Information (http://www.blast.ncbi.nlm.nih.gov/). According to the extent of similarity to the reference DNA sequences on the database, the taxonomy of the bacterial isolate was identified.

Table 3. 2   Universal primer sequences used for complete sequencing of 16S rRNA gene

Primer	Sequences (5' to 3')	Reference
8F	AGA GTT TGA TCC TGG CTC AG	[79, 80]
1512R	GGY TAC CTT GTT ACG ACT T	[79, 80]
902F	GGT TAA AAC TYA AAK GAA TTG ACG G	[79, 81, 82]
1391F	TTG YAC ACA CCG CCC GTC	[79, 82]
519F	CAG CMG CCG CGG TAA TWC	[81]
536R	GWA TTA CCG CGG CKG CTG	[81]
363R	CTG CTG CCT CCC GTA GG	[83]
Y(C, T); M(A, C); K(G, T); W(A, T)		

Table 3. 3   PCR reaction components for 16S rRNA gene

Component	Volume (μl)	Final concentration
10X Taq buffer	5	1X
2.5 mM dNTP	2	0.1 mM
10 μM forward primer (8F)	1	0.2 μM
10 μM reverse primer (1512R)	1	0.2 μM
Taq DNA polymerase	0.5	1 unit
Sterile distilled water	40.5	---
Total volume	50	---

3.3 Batch experiments for NDMA biotransformation capability screening on the bacterial isolates

Single colony taken from the isolate on the R2A agar plate was inoculated into 30 ml of R2A medium amended with 10 μg/L of NDMA and incubated at 25℃ for 5 days to the late exponential phase of growth (OD$_{600}$ ~ 0.6-1.0). The cells were harvested by centrifugation at 8,000 rpm for 5 minutes and resuspended the cellular pellet in 2 ml of nitrogen-free basal salt medium (BSM, Table 3. 4). Each pure culture suspension was divided into two aliquots. After centrifuging at 13,000 rpm for 5 minutes, the supernatant was discarded to remove additional R2A medium. The cells were resuspended in 10 ml of R2A medium or BSM containing 1 mg/L of NDMA, respectively. This screening experiment was performed at 25℃ for 28 days, and the NDMA analysis was conducted every 7-day.

Table 3. 4   Basal salt medium (BSM) components

Component	Concentration (mM)
$MgSO_4 \cdot 7H_2O$	0.15
$FeSO_4 \cdot 7H_2O$	0.04
$CaSO_4 \cdot 2H_2O$	0.05
H_2SO_4	0.1
H_3BO_3	0.002
$MnSO_4 \cdot H_2O$	0.002
$ZnSO_4 \cdot 7H_2O$	0.002
KI	0.001
$CoCl_2 \cdot 6H_2O$	0.0043
KH_2PO_4	3.9
Na_2HPO_4	6.1

3.4   NDMA analysis

For NDMA analysis, 1 ml of sample was removed from the culture suspension and 1 μl of 85% phosphoric acid was added to inhibit the bioactivity. The mixtures were centrifuged at 13,000 rpm for 30 seconds, and the supernatants were passed through a nylon filter (Critical, Nashua, USA) with 0.45 μm pore size and placed in 2-ml amber glass vials. NDMA was analyzed with a high pressure liquid chromatography (HPLC) system (1200 series, Agilent Technologies, CA, USA) with a diode array detector (DAD) at 230 nm. Separations were performed in a Eclipse Plus C18 column (5 μm pore size,

4.6 x 150 mm, Agilent Technologies, CA, USA), and the mobile phase was the mixture of

97.5% (v/v) of phosphate buffer (pH 2.0) and 2.5 % (v/v) of 99.9% methanol at constant

flow rate of 1 ml/min (Table 3. 5). Calibration curves were prepared for each sample

batch.

Table 3. 5   Instrument conditions and materials for NDMA analysis

HPLC coupled to Diode Array Detector (DAD)

HPLC system	1200 series, Agilent Technologies, CA, USA
LC column	C18, 5 μm pore size, 4.6 x 150 mm
Injection volume	10 μl
Mobile phase	97.5% (v/v) of 2 mM KH_2PO_4 and 35.8 mM H_3PO_4 (pH 2.0), 2.5% (v/v) methanol
Flow rate	Constant flow rate of 1 ml/min
Run time	10 min
Retention time	3.7 min
Detector	Diode array detector with 230 nm absorbance
Method detection limit	3.1 μg/L

3.5   Characterization of the pure bacterial isolates

3.5.1   Nitrogen and carbon sources

Growth test was performed on the bacterial isolates grown with NDMA as nitrogen

and/or carbon source. Sufficient carbon and nitrogen sources were provided at the ratio

of 5 to 1, based on the general constituents of cellular biomass [84]. Descriptions for the design of the growth tests and four sets of negative controls were summarized in Table 3. 6. Initially, pure bacterial glycerol stocks were inoculated in 200 ml of R2A medium amended with 0.1 M of methanol and 13.5 μM (1 mg/L) of NDMA. After 29 hours of pre-incubation at 25℃, the cells were harvested by centrifugation at 3,000 rpm for 5 minutes and washed three times by nitrogen-free BSM. An 8-ml of nitrogen-free BSM was added to resuspend the cellular pellet and then the suspension was divided into 8 aliquots. Five of them were tested for growing on 2.1 mM nitrate (Batch 5), 2.1 mM ammonium (Batch 6), 20 mM NDMA as sole nitrogen and carbon sources (Batch 7), 2.1 mM NDMA as nitrogen source (Batch 8), or 20 mM NDMA as carbon source (Batch 9), respectively. The rest cell aliquots were added into three negative controls as described as Table 3. 6 (Batch 1, 2, 4). Batch 3 was a sterile control without bacterial cells added. In this experiment, all serum bottles used were covered by aluminum foil to avoid photodegradation of NDMA. The pure bacterial cells were incubated at 25℃ with shaking at 150 rpm during the growth tests. A 3-ml volume of samples were removed from each bottles daily, 1-ml of samples was used for OD measurement, and the rest were used for duplicate NDMA analysis.

Table 3. 6　　Growth substances test and cometabolic experiment designs

Purpose of batch design	Initial cell conditions	Carbon source	Nitrogen source	NDMA addition
1. Negative control --- without nitrogen source	Presence	Methanol	---	No
2. Negative control --- without carbon source	Presence	---	NO_3^- and NH_4^+	No
3. Negative control --- without bacterial cells	Absence	Methanol	NO_3^- and NH_4^+	Yes
4. Negative control --- NaN_3 treatment	Inactivated	Methanol	NO_3^- and NH_4^+	Yes
5. Positive control --- nitrate as nitrogen source	$OD_{600} < 0.1$	Methanol (10 mM)	NO_3^- (2.1 mM)	No
6. Positive control --- ammonium as nitrogen source	$OD_{600} < 0.1$	Methanol (10 mM)	NH_4^+ (2.1 mM)	No
7. Growth test --- NDMA as sole carbon and nitrogen source	$OD_{600} < 0.1$	NDMA (10 mM)		Yes
8. Growth test --- NDMA as sole nitrogen sources	$OD_{600} < 0.1$	Methanol (10 mM)	NDMA (2.1 mM)	Yes
9. Growth test --- NDMA as sole carbon sources	$OD_{600} < 0.1$	NDMA (10 mM)	NO_3^- and NH_4^+ (1.05 mM each)	Yes
10. Cometabolic experiment --- methanol amended	$OD_{600} \sim 0.2$	---	---	1 mg/L
11. Cometabolic experiment --- without methanol amended	$OD_{600} \sim 0.3$	---	---	100 μg/L

3.5.2   Cometabolic effect experiment

This experiment was designed to determine whether the bacterial isolates had the ability to degrade NDMA via cometabolism. Descriptions for the design of cometabolic experiments and two sets of negative controls were also summarized in Table 3. 6. Pure bacterial glycerol stocks were grown in 200 ml of R2A medium amended with 0.1 M of methanol and 1 mg/L of NDMA at 25℃. During the mid-exponential phase (OD_{600}~0.3-0.5), the cells were harvested by centrifugation at 3,000 rpm for 5 minutes and washed three times by nitrogen-free BSM. After discarding the supernatant, cells were divided into 3 aliquots. One aliquot was grown on BSM amended with 2.1 mM of ammonium and 10 mM of methanol (Batch 10). The second aliquot was transferred to the phosphate buffer solution (PBS, Table 3. 7) (Batch 11). Negative controls consisted of sterile control (Batch 3) and the third cell aliquots treated with 4.6 mM of sodium azide (Batch 4). The media used for negative controls were the same as experimental sets. Next, NDMA (1 mg/L or 100 µg/L) was added into the cell suspensions, and all of the serum bottles used was covered by aluminum foil to prevent NDMA from photodegradation. The cell cultures were incubated at 25℃ with shaking at 150 rpm for the degradation of NDMA. In the beginning, 2 ml of cellular suspension was taken for methanol analysis (section 3.5.3). A 3-ml volume of samples were removed from each

bottles at the pre-scheduled time, 1-ml of samples was used for OD measurement, and the rest was used for duplicate NDMA analysis.

Table 3. 7   Phosphate buffer solution (PBS) components

Component	Concentration (g/L)
NaCl	8
KCl	0.2
Na_2HPO_4	0.61
KH_2PO_4	0.2
pH~7.3	

3.5.3   Methanol analysis

For methanol analysis, 2 ml of sample was removed from the culture suspensions and 2μl of 460 mM sodium azide was added to inhibit the bioactivity. The mixtures were then passed through a Nylon filter (Critical, Nashua, USA) with 0.45 μm pore size and placed in 2-ml amber glass vial. Methanol was analyzed using gas chromatographic (6890N, Agilent Technologies, CA, USA) - mass spectrometry (5973N, Agilent Technologies, CA, USA) with purge-and-trap (Eclipse 4660, OI corporation, Texas, USA) pretreatment. Separations were performed on an Rtx-Volatiles capillary column with 60 m long by 0.32 mm I.D. and 1.5 μm thickness (Restek corporation, USA), and the operation parameters were shown as Table 3. 8. Methanol analysis was accomplished

in one day. The instrument detection limit (IDL) was about 0.046 mM (1.47 mg/L).

Table 3. 8　Operation parameters for methanol analysis by GC/MS

Purge and Trap pretreatment

Process	Operation parameters
Purge	Constant flow at 40 ml/min by high purity nitrogen gas for 11 minutes
Dry purge	Constant flow at 200 ml/min by high purity nitrogen gas for 1 minutes
Desorb	Constant flow at 300 ml/min by high purity nitrogen gas for 4 minutes at 270℃
Bake	Constant flow at 300 ml/min by high purity nitrogen gas for 10 minutes at 280℃

Gas chromatograph

Carrier gas and flow rate	Nitrogen gas, constant flow at 8 ml/min
Injection port temperature	200 ℃
GC temperature conditions	40℃ held for 4 minutes, and then ramping at 6℃/min to 200 ℃

3.6　Kinetic study of NDMA biotransformation

3.6.1　Batch experiment designs

Pure bacterial glycerol stocks were grown in 400 ml of R2A medium with stirring at 25℃. During the late-exponential phase (OD_{600}~0.5-0.6), the cells were harvested by centrifugation at 3,500 rpm for 20 minutes and washed once by BSM (20 mM NH_4Cl added). Followed by discarding supernatant completely, cellular pellet was resuspended

in BSM containing NDMA. Two negative controls were used to verify no abiotic effects were involved in these experiments, one is sterile control without bacterial cells and the other was treated with 4.6 mM sodium azide to inhibit cellular activity. All serum bottles used were sterilized before the tests and were covered with aluminum foil to prevent the NDMA from photodegradation.

For temperature effect experiments, the initial NDMA concentration was set at 50 µg/L, 100 µg/L or 600 µg/L. Cell cultures were incubated at 15℃, 25℃, and 35℃, respectively, with shaking at 130 rpm for degradation of NDMA.

In order to assess the feasibility of NDMA biotransformation in the full scale slow sand filter, the 0.22 µm filtered sterile influent from slow sand filter was spiked into the incubation media at different proportions, including 10%, 50%, and 100%, and then NDMA (100 µg/L) was added. Cell cultures were incubated at 25℃ with shaking at 130 rpm.

Mixed bacteria conditions were constructed to extend the observation of NDMA biotransformation from pure bacterial culture to mixed bacterial cultures. Two kinds of mixed cultures were generated. First, the three bacterial isolates were inoculated separately and then combined together (referred as mixed cultures amended in figure legends); second, the four bacterial isolates were inoculated together for subculture (referred as mixed subcultures in figure legends).

All kinetic experiments were conducted in duplicate. At the beginning, a 4 ml

volume of samples were taken from each bottle, 1 ml of samples was used for OD

measurement, another 1 ml of sample was used for NDMA analysis, and the rest was

used for the protein measurements. Then, at each scheduled time, 1 ml of samples was

taken and analyzed for the residual NDMA in the solution.

3.6.2   Protein measurements

A 2 ml aliquot of sample was taken from the bacterial suspensions and centrifuged

at 13,000 rpm for 10 minutes to discard the medium. Cells were disrupted in 0.1 N

NaOH solution at 80℃ for 10 minutes, and then 10 minutes of centrifugation was

conducted to collect the supernatant containing cellular proteins. Quantification of

proteins was accomplished by the BCA Protein Assay Kit (Novagen, Darmstadt,

Germany).

3.7   Continuous acclimation culture

3.7.1   Column establishment and sampling

A simulated sand column system was setup in the laboratory for the purpose of

acclimation of NDMA-degrading bacteria and spatial distribution of microorganisms

along the sand column. All of the materials used were tested for NDMA adsorption

incapability prior to use. The column was constructed by 4 sections of polyvinyl

chloride (PVC) cylinders with 2-cm diameter and the total height of the column was 1

m. Sand samples from Kinmen were then filled into the laboratory simulated column, and water samples from influent of full scale slow sand filter were used to stabilize the bacterial community at constant flow of 1 ml/min by a tubing pump. After 5 days contact time for stabilization, 100 μg/L of NDMA was spiked into the influent of the laboratory column. During the 268 days operation, column influent and effluent samples were collected and analyzed for NDMA, non-purgeable dissolved organic carbon (NPDOC), or dissolved organic nitrogen (DON). NPDOC and DON analysis were accomplished in one day.

3.7.2   Non-purgeable dissolved organic carbon (NPDOC) analysis

Samples for NPDOC analysis were filtered through a 0.45 μm pore size of cellular membrane to remove particles. A 5 ml volume of samples were transferred to a glass tube and 2 drops of 2 N HCl were added to adjust the pH to lower than 2. After acidification, inorganic carbon will be transformed into carbon dioxide and purged before analysis.

NPDOC were measured by a TOC 5000A total organic carbon analyzer (Shimadzu, Kyoto, Japan) with model ASI-5000 auto sample injector (Shimadzu, Kyoto, Japan). Samples were purged with air for 3 minutes to remove gaseous CO_2 and 80 μl samples were analyzed after high temperature combustion (Standard Method 5310B) [85] and the concentration of CO_2 is quantified by a non-dispersive infrared detector.

3.7.3 Dissolved organic nitrogen (DON) analysis

DON concentration were determined by subtracting total dissolved inorganic nitrogen species, including nitrate (NO_3^--N), nitrite (NO_2^--N) and ammonium (NH_4^+-N), from TDN. Samples for TDN, nitrate, nitrite and ammonium analysis were filtered through a 0.45 μm pore size of cellulose membrane (Millipore, Carrigtwohill, Co Cork, Ireland) to remove particles.

The TDN analysis followed the methods conducted by Wang *et. al*. [86]. Nitrate stock solution (1000 mg/L as nitrogen) was used for calibration curve preparation. All the materials used for the TDN analysis were shown in Table 3. 9. A 5 ml volume of samples were transferred to the heat-resistant glass tube with Teflon-lined screwed cap and 0.5 ml of alkaline $K_2S_2O_8$ solution was added and then autoclaved at 121℃ for 60 minutes. After cooled down to the room temperature, 1-ml samples were transferred to test tubes containing 4-ml of sulfuric and phosphoric acid mixture, and 0.2 ml of 2, 6-dimethylphenol was added. Followed by cooling down at 20℃ for 15 minutes, TDN concentration was measured by the absorbance at 337 nm using spectrophotometer (UV-160A, Shimadzu corporation, Japan).

Nitrate analysis was according to the Standard Method 4110B [85] by ion chromatography system (Model Dx-120, DIONEX, CA, USA) equipped with an auto sampler (Model AS100, SpecTRASeries, CA, USA) and the ion exchange was

performed on a IonPacRA54A column (4 x 150 mm) (DIONEX, CA, USA). The eluent solution consisted of 1.8 mM Na_2CO_3 and 1.7 mM $NaHCO_3$. Because high concentration of chloride would hinder the signals of nitrate anion, samples containing chloride were passed through an onGuard®II Ag cartridge (DIONEX, CA, USA) to remove the interference. The system was equilibrated to 2 ml/min of the eluent flow rate and 1600-2300 psi with nitrogen gas before analysis. Each sample was analyzed for 7 minutes and the concentration was determined by the peak height as well as calibration curve.

The colorimetric method for nitrite analysis was based on the Standard Method 4500- NO_2^--B [85]. A color reagent was prepared by adding 100 ml of 85% phosphoric acid to 800 ml deionized water to dissolve 10 g of sulfanilamide completely, and then 1 g *N*-(1-naphthyl)-ethylenediamine dihydrochloride was added to the mixture and diluted to 1 L. Five ml volume of sample was combined with 0.2 ml color reagent and stood for 30 minutes at room temperature. Absorbance at 543 nm was then measured by spectrophotometer for NO_2^- quantification.

Ammonium concentration was determined using a commercial kit (Spectroquant®, MERCK, Darmstdt, Germany) for transformation of ammonium to monochloramine. Aliquots of thymol solution were added with the monochloramine to form a blue-color complex, and the absorbance at 690 nm was measured with a spectrophotometer.

Table 3. 9   Reagents for TDN analysis

Reagent	Preparation
Nitrate stock solution	1000 mg/L as nitrogen
Alkaline $K_2S_2O_8$ solution	148 mM in 0.375 N NaOH
Sulfuric and phosphoric acid mixture	$H_2SO_4 : H_3PO_4 = 3:2$ (volume ratio)
2,6-dimethylphenol	122.8 mM in 30% isopropylalcohol

3.8   Microbial distribution in the field and the simulated sand column

3.8.1   Genomic DNA extraction

The microbial genomic DNA extracted from sand samples was isolated according to the protocol described by Easy Pure Genomic DNA purification kit (Bioman, Taiwan) for gram-positive bacteria with some modifications to improve DNA recovery efficiency. In general, 50 g of wet sand samples was added to the 30 ml sterile 1X PBS. The sample was first sonicated for 10 minutes and vortexed for 5 seconds. Subsequently, the sample was settled for 10 minutes and the supernatant was transferred into a sterile 50-ml centrifuge tube. This procedure was repeated twice to detach most microorganisms on sand surface, and the microorganisms were collected by centrifugation at 14,000 xg for 2 minutes. The pellet was resuspended with 1X PBS and transferred to a 2-ml eppendorf tube, and then centrifuged at 14,000 xg for 2 minutes to remove the supernatant. After

washed twice by 1X PBS, the pellet was resuspended thoroughly in 120 µl of 10 mg/ml

lysozyme and 480 µl of 50 mM EDTA and incubated at 37℃ for 1 hour. The cells were

lysed by adding 600 µl of Cell Lysis Solution with gently pipetting, and additional

incubating at 80℃ for 10 minutes. Next, the cell lysate was treated with 3 µl of RNase

solution and inverted the eppendorf gently for 10 times and incubated at 37℃ for 1

hour to remove the RNA molecules. After cooled down to room temperature, 200 µl of

Protein Precipitation Solution was added and followed by vortexing vigorously for 20

seconds. The mixture was placed on ice for 5 minutes and then centrifuged at 14,000 xg

for 3 minutes. The supernatant was transferred to another 2 ml eppendorf tube which

contained 600 µl of isopropanol and inverted the eppendorf gently for 10 times. To

increase the DNA recovery, the samples were placed at -20℃ for 15 minutes and

centrifuged at 14,000 xg for 2 minutes. After carefully removed the supernatant, the

DNA pellet was rinsed with 600 µl of 70% ethanol by gently inverting the tube and then

retaining the DNA by centrifugation at 14,000 xg for 2 minutes and poured the

supernatant off. The extracted DNA was vacuum-dried and rehydrated in 100 µl of

DNA Rehydration Solution at 65℃ for 1 hour. For complete rehydration, the eppendorf

tube was periodically tapped. The impurity in DNA sample was further removed using a

commercial Wizard DNA Clean-Up system (Promega, USA), according to the protocols

provided. Finally, the DNA was redissolved in 30 µl of sterile distilled water and stored

at -20℃ for later used.

3.8.2 Complete sequencing of 16S rRNA gene

The 16S-rRNA gene sequence of bacterial isolates was determined by automatic sequencing (Genomics BioSci & Tech, Inc., Taiwan) as described at section 3.2.3. Several primers as shown in Table 3. 2 were designed for the conservative region of 16S rRNA gene. After amplifying the 16S rRNA gene, these primers were used to determine partial sequences among the 16S rRNA gene, respectively. The complete nucleotide sequence was analyzed with a CLC main workbench program (CLC bio, version 5.6.1, 2009) to assemble these sequencing data into an intergrated sequence.

3.8.3 Terminal Restriction Fragment Length Polymorphism (T-RFLP)

For pure culture strains and DNA extracted from sand samples, 16S rRNA gene was amplified as described at section 3.2.3. However, the forward primers (8F) used for T-RFLP methods was designed as 5'-FAM fluorescent dye labeled oligonucleotides. After PCR amplification, reagents containing residual nucleotides, primers and salts were removed using an Easy Pure PCR clean up kit (Bioman, Taiwan) based on the manufacturer's instructions.

PCR products were concentrated according to the ethanol precipitation methods described on The Condensed Protocols from Molecular cloning [78]. The 5 M NaCl stock solution and 95% ethanol were added to the cleaned PCR products to achieve the

52

final concentration of 0.28 M and 63%, respectively. The mixture was then placed at -20

℃ for over 16 hours to precipitate the DNA. Next, the DNA pellet was obtained by

centrifugation at 14,000 xg for 30 minutes at 0℃ and the supernatant was carefully

discarded. Subsequently, the precipitated DNA was washed with 70% ethanol and

followed by centrifugation at 14,000 xg for 10 minutes at 0℃ to remove salts,

vacuum-dried in a Speedvac concentrator (Thermo, USA) and finally redissolved in 30

μl sterile distilled water.

Concentrated PCR products were double-digested by 10 and 15 units of restriction

enzymes, *Rsa*I and *Xma*I (NEB, Ipswich, UK), respectively. The reagents of restriction

enzyme digestion were shown in Table 3. 10. After incubation at 37℃ for 90 minutes,

the enzymes were inactivated by heat treatment at 65℃ for 20 minutes. All of the

reaction products in this section were checked by 1.5% agarose gel electrophoresis. The

different lengths of terminal restriction fragments (T-RFs) were resolved by capillary

electrophoresis coupled to a fluorescence detector (Tri-I Biotech, Inc., Taiwan) for

relative quantification. The fragments between 75 and 550 bp corresponding to the size

range of the standard were then determined.

Table 3. 10 The reagents used for restriction enzyme digestion

Component	Volume (μl)	Final concentration
Concentrated PCR product	10	0.5 μg to 1 μg
10X NEBuffer 4	3	1X
100X BSA	0.3	100 μg/ml
*Xma*I	1.5	15 units
*Rsa*I	1	10 unit
Sterile distilled water	14.2	---
Total volume	30	---

Chapter IV   Results and Discussion

4.1   Isolation and identification of bacteria from the biofilm on sand surface

4.1.1   Isolation and growth curve of bacterial isolates

Four pure bacteria cultures were isolated from the biofilm of slow sand filter. The morphology of these isolates was shown in Figure 4. 1. The colony of isolate A, B, and C were circular with yellow, white, and pink color, respectively. Isolate D formed white-color, circular-shaped with wavy margin colonies.

The growth of isolate A and D were faster than isolate B and C at 25℃. Growth curves showed that mid exponential phase could be achieved before 20 hours for the isolate A and D, but were 30 and 50 hours for isolate B and C, respectively (Figure 4. 2). In addition, the cell density of isolate A and D could reach the absorbance at 600 nm (OD_{600}) of 1~1.2, but for isolate B and C, the maximal growth density were 0.6~0.8 at OD_{600}. For liquid cultivation, isolate C would aggregate when growing to higher density.
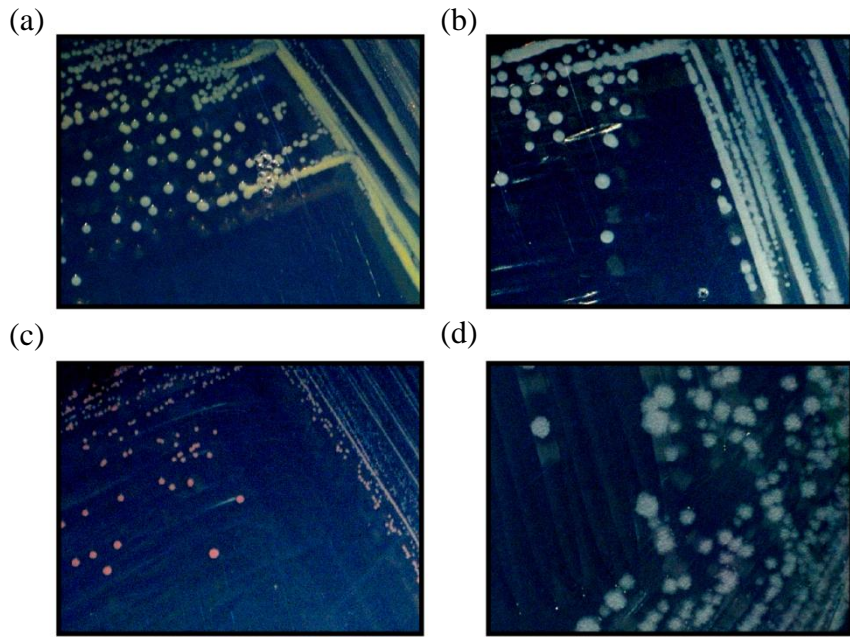
Figure 4. 1   Photographs of isolated bacteria pure cultures from field sand on the R2A

agar plate. (a) Isolate A. (b) Isolate B. (c) Isolate C. (d) Isolate D.
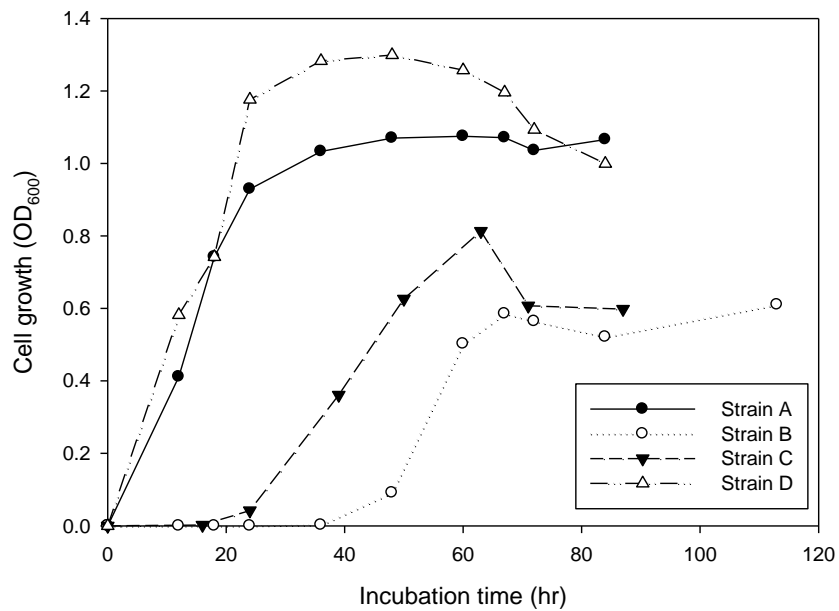
Figure 4. 2   Growth curves of isolated bacteria pure cultures from field sand.

4.1.2 Phylogenetic identification of bacterial isolates

In the section, the identification of these four isolates from slow sand filter was according the similarity of the sequences to the GenBank database by nucleotide Basic Local Alignment Search Tool (BLAST). The results were shown in Table 4. 1.

Isolate A belonged to genus *Sphingomonas*, which included many strictly aerobic, chemoheterotrophic, and gram-negative yellow-pigmented bacteria [87]. These bacteria could be found from various environments, such as freshwater, seawater, soil, and drinking water supplies. The most noticeable property is the ability to degrade a wide range of xenobiotics with aromatic rings, including bisphenol A, bisphenol F [88], nonylphenol [89], aromatic hydrocarbon [90].

Isolate B was the member of genus *Terrabacter*, which was reclassified from the genus of *Pimelobacter* [91]. The former could be differentiated from the latter on the compositions of cell walls [92]. From the phenotypic characterization, the members of genus *Terrabacter* were strictly aerobic, non-motile, gram-positive bacteria, and with white, convex, circular and entire margin appearance. The genus *Terrabacter* could be found in soil, stone, air samples [92-94].

Isolate C was identified as the member of genus *Methylobcterium*, a group of strictly aerobic, gram-negative, rod-shaped, facultatively methylotrophic bacteria [95]. Because of the production of carotenoids, the cultures presented the color of pink to red

and was called as pink-pigmented facultatively methylotrophic (PPFM) bacteria. Under

aerobic growth condition, some of them have the photochemical reaction system as

purple phototrophic bacteria, so that they were classified as the phototrophic bacteria.

The *Methylobacterium* species were able to grow on single-carbon compounds such as

methanol, formate, or formaldehyde as the sole source of carbon and energy, or on

various multi-carbon compounds [95]. The aggregating phenotype of isolate C (section

4.1.1) at higher density could be attributed by cell-to-cell signals. Poonguzhali *et al.* [96]

reported that the production of a cell-to-cell signaling molecule, *N*-acyl-homoserine

lactone (AHL), was detected in most of the *Methylobacterium* species. This

phenomenon was known as quorum sensing, and the synthesis of this compound was

cell-density dependent, often during the late exponential to stationary phase. The

members of genus *Methylobaterium* were found in a variety of habitats because of their

ubiquity in nature. They could exist in soil, seawater, freshwater, tap water systems, lake

sediments, dust, leaf surfaces, air, or as contaminants in many products and manufactory

processes [95, 97, 98]. Most of the *Methylobacterium* sp. isolated from environments

were highly resistant to chlorine [99], therefore, these strains were found occurrence in

the chlorinated environments frequently.

Isolate D was a member of genus *Bacillus*, which could be aerobic or facultatively

anaerobic spore-forming bacteria with rod shape [100]. Most species of the genus

Bacillus were gram-positive bacteria, but some were gram-variable. This genus

contained several types of species, which were thermophilic or psychrophilic, but most

could grow at the optimal temperature range from 25℃ to 37℃ [100]. They were

ubiquitous in the environment, and many species of genus *Bacillus*, especially *B. cereus*,

caused two types of food poisoning or clinical infections. Therefore, studies concerning

the detection from foodstuffs or clinical samples and identification of toxins had arisen

[101, 102].

Table 4. 1   Phylogenic analysis of isolates on nucleotide BLAST database

	Isolate A	Isolate B	Isolate C	Isolate D
Blast result	*Sphingomonas* sp.*,* strain: SZL-1	*Terrabacter tumescens*, type strain: KCTC* 9133	*Methylobacterium lusitanum*, strain: MP2	*Bacillus cereus*, strain: HLSSD-5
Accession number	FJ158842	AF005023	EF015479	FJ749283
Identity	99%	99%	99%	100%
Source	Soil, sediment	Soil, stone, air	Tap water, soil	Soil
Characteristics	Triazophos degradation	Resistance to environmental hazards	Facultative methylotroph	PAH degradation
References	[88-90, 103, 104]	[92-94]	[96, 97, 99, 105]	[100, 101]

* KCTC, Korean Collection for Type Cultures.

4.2 NDMA bio-reduction capability screening on bacterial isolates

To test for the capability of NDMA bio-reduction among pure cultures isolates, each isolate was incubated in R2A medium amended with 10 µg/L NDMA initially until late exponential phase and transferred to nitrogen-containing basal salt medium (N-BSM) or R2A medium with presence of 1 mg/L NDMA. The initial cell density of all isolates was ranging from 0.6 to 0.8 (OD_{600}). The bottles were covered with light shield to prevent photodegradation of NDMA.

The results demonstrated that isolate A and B could only reduce a small fraction of NDMA throughout the screening test (Figure 4. 3). The percentage of NDMA reduction in N-BSM for 28 days incubation was only 20% for both isolate A and B. Similar results were observed in R2A medium as the NDMA was decreased by 20% and 32% for 28 days incubation for isolate A and B, respectively. However, rapid reduction of NDMA concentration was observed by isolate C and D, which belonged to the members of *Methylobacterium* and *Bacillus* species, respectively. NDMA was not detectable after 28 days incubation in N-BSM or 7 days in R2A medium by isolate C, but there were 46% and 89% NDMA remaining in the system when incubated with isolate D. The results indicated that both isolate C and D had the ability to reduce NDMA, but the efficiency by isolate C was higher than isolate D. In this screening experiment, lack of negative controls caused an uncertainty of other abiotic effects on NDMA, such as adsorption by

extracellular materials, but significant differences observed between four isolates might suggest that biological effects were indeed happened by isolate C and D. In N-BSM, no significant growth was observed during 28 days incubation for isolate C and D; in contrast, the OD_{600} of the bacterial cell cultures grown in R2A medium could reach to 1~1.5, some with aggregations. Thus, NDMA was assumed not a carbon source for the microorganisms. Other experiments were conducted to confirm the carbon and nitrogen sources for isolate C (section 4.3).

(a)

N-BSM amended with NDMA

(b)

R2A amended with NDMA
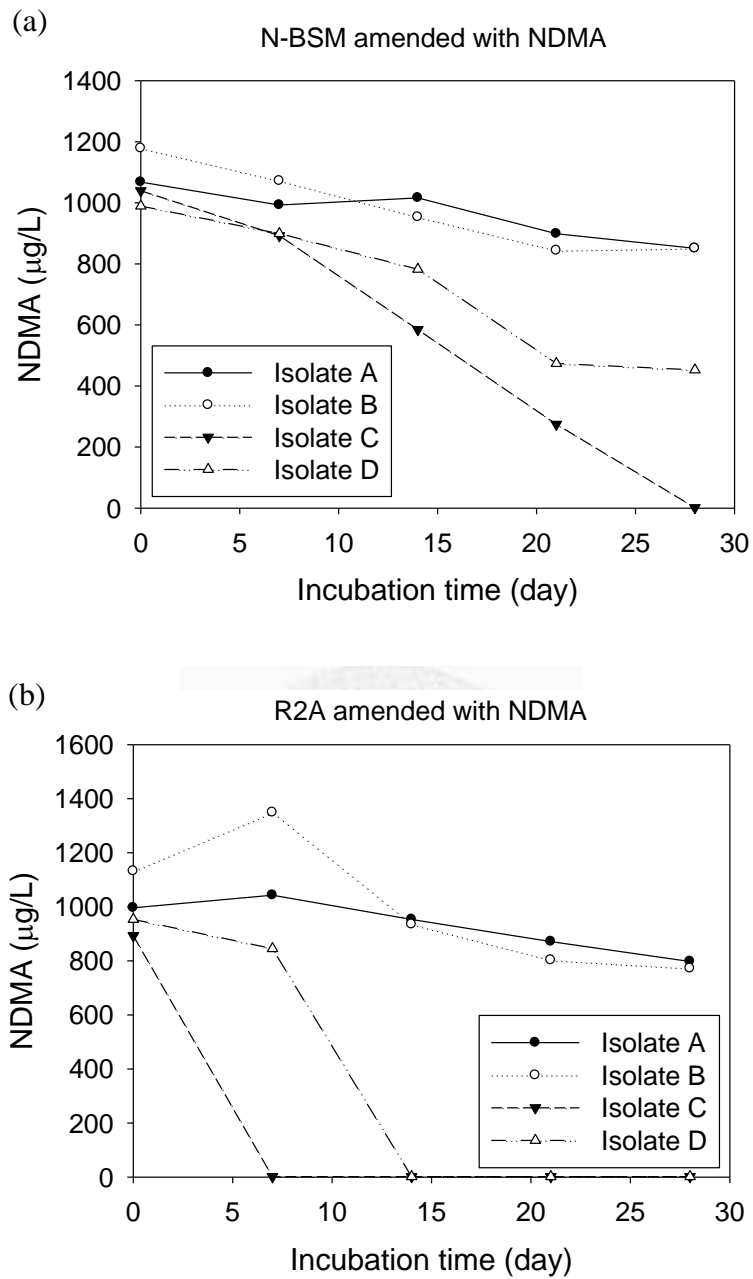
Figure 4. 3   NDMA concentrations in screening experiments. (a) In nitrogen-containing basal salt medium (N-BSM). (b) In R2A medium amended with NDMA.

4.3　Characterization for the isolate of *Methylobacterium* sp.

The metabolic characteristics of the *Methylobacterium* sp. isolate were investigated. The experiments were set up to explore whether the isolate utilized NDMA as the carbon energy source, nitrogen source. The bacterial isolate was first incubated in R2A amended with methanol, and subsequently transferred to different media combination (Table 3. 6) at low cell density (OD_{600}~0.1) for further growth tests. Sufficient carbon and nitrogen sources were provided at the ratio of 5 to 1, based on the general constituents of cellular biomass [84]. In addition, the isolate of *Methylobacterium* sp. was capable of sustained growth to the cell density more than 0.5 (OD_{600}) (Figure 4. 2) under sufficient growth sources, therefore, the increase of cell density from 0.1 to 0.5 (OD_{600}) was considered as detectable growth. Detectable NDMA reduction is identified as more than 10% of NDMA disappeared throughout the experiment.

Since the isolate of *Methylobacterium* sp. was a facultative methylogen, methanol was used as the sole carbon source in growth tests. Previous researches demonstrated that most bacteria could use ammonium (NH_4^+) as inorganic nitrogen source, and many are capable of utilizing nitrate (NO_3^-) as well [84]. For the isolate of *Methylobacterium* sp., significant growth (OD_{600} more than 0.5) was observed while growth on nitrate (Batch 5) or ammonium (Batch 6) as nitrogen source (Table 4. 2), but cells grew in nitrate containing media formed aggregations when cell density was high.

64

No detectable growth was observed in the absence of either nitrogen source (Batch 1) or carbon source (Batch 2), revealing no other growth substances existed in the batch experiment. In the control groups, Batch 3 and 4, no detectable growth or NDMA degradation were found. This confirmed that there were no abiotic losses of NDMA during the test. In Batch 7, NDMA was used as the only carbon and nitrogen source, but no detectable growth was observed in 7 days incubation, in addition, NDMA remained as the initial concentration throughout the incubation period. The same results were found in Batch 8 and Batch 9, which replaced nitrogen source (ammonium/nitrate) or carbon source (methanol) with NDMA, respectively. Based on the results shown in Table 4. 2, the *Methylobacterium* sp. isolate was not able to use NDMA as sole carbon and nitrogen source. This was in consistent with previous studies showed that no bacteria was found to use NDMA as the sole carbon source for cell growth [10, 55, 56], even NDMA was mostly mineralized to CO_2 by microorganisms according to the isotope tracer studies [10, 12]. However, Fournier *et al.*(2009) recently found that propanotroph *Rhodococcus ruber* ENV425 could utilize NDMA as well as many NDMA degradation intermediates as nitrogen source when growing on propane [56].

Table 4. 2   Growth tests for the isolate of *Methylobacterium* sp.

Batch[+]	Growth substance		Detectable growth*	Detectable NDMA reduction[#]
	Carbon source	**Nitrogen source**		
1	Methanol	---	No	---
2	---	NO_3^- and NH_4^+	No	---
3	Methanol	NO_3^- and NH_4^+	No	No
4	Methanol	NO_3^- and NH_4^+	No	No
5	Methanol	NO_3^-	Yes	---
6	Methanol	NH_4^+	Yes	---
7	NDMA	NDMA	No	No
8	Methanol	NDMA	No	No
9	NDMA	NO_3^- and NH_4^+	No	No

+ Batch designs are described in Table 3. 6.

* Detectable growth denotes optical density (OD_{600}) more than 0.5.

Detectable NDMA reduction is identified as more than 10% of NDMA disappeared throughout the experiment.

From the above substrate utilization experiments, NDMA could not be used as neither carbon nor nitrogen source. The mechanism of NDMA bio-reduction by isolate *Methylobacterium* sp. was further explored through the cometabolism process, as reported by previous studies [53-56]. In the cometabolic experiments, it was assumed that either R2A or methanol was the inducing substrate which stimulated the production of NDMA-reducing enzymes. Therefore, the bacterial isolate was initially grown on R2A medium amended with methanol to the mid-exponential phase. Then, cells were washed three times by nitrogen-free BSM to remove extra medium.

The results revealed that washed cells grew rapidly in the presence of methanol (10 mM), and then reached to the density saturation after four days as the results of nutrient depletion (methanol< 0.046 mM) and toxic accumulations (Figure 4. 4 a). NDMA concentration started to decrease after four days of incubation (Figure 4. 4 b), which was coincided with the time cell growth ceased. About 30 percent of NDMA was reduced after 10 days incubation. It is possible that the bacterial isolate would favor to sustain growth on the primary substrate, methanol in this case, instead of metabolizing NDMA.

Figure 4. 5 shows that NDMA was rapidly decreased after 1 day in absence of methanol, and these results also supported our speculations above. Without growth substrates (methanol< 0.046 mM), the isolate of *Methylobacterium* sp. would act on the NDMA quickly. Besides, three times washed by BSM might result in longer periods of

cell adaptation and reflected on the one-day lag time to NDMA reductions.

Combined with the results demonstrated in section 4.2 and 4.3, suggesting that NDMA was not a carbon and/or nitrogen sources for cell growth, but reduce NDMA through cometabolic process happened when limited nutrients were provided. However, in section 4.2, NDMA was reduced when cell growth on R2A medium. It is because much higher initial cell numbers (OD_{600} ~ 0.6-0.8) were involved in the screening experiment, so that would result in unequal distribution of nutrients for the cell cultures. In the real situations which were oligotrophic environments and with low cell numbers, we suggested that NDMA bio-reduction is possible.

There were several studies providing evidences regarding different monooxygenase enzymes responsible for NDMA cometabolic biodegradation, which were induced by organic matters, such as methane, propane or toluene [53, 54]. To confirm the inducing substrates for NDMA-degrading enzymes expressed by the isolate of *Methylobacterium* sp., R2A and/or methanol were tested as the carbon and energy sources for NDMA cometabolism. Three sets of experiments were constructed individually. Except for the methanol only, the *Methylobacterium* sp. isolate reduced NDMA to the undetectable levels after growth on R2A medium or R2A medium amended with methanol (Figure 4. 6). The results suggested that the complex nutrients, R2A, could serve as an inducing substrate for enzymes involving in the NDMA

bio-reduction by the isolate of *Methylobacterium* sp..

The organic substances in R2A medium were including yeast extract, proteose peptone, casamino acid, dextrose, starch and sodium pyruvate (Table 3. 1). Among them, yeast extract, proteose peptone and casamino acid were complex matrix, which primarily consisted of many amino acids or peptides. In contrast, dextrose, starch and sodium pyruvate were pure compounds, which belonged to the carbohydrates involving in the process of cellular respiration for ATP production [106]. Therefore, the possible inducing substrates for expressing enzymes responsible for NDMA reduction might be one of the amino acids or peptides in the mixtures, which could act as transcriptional factors or signaling molecules directly.

(a)

(b)
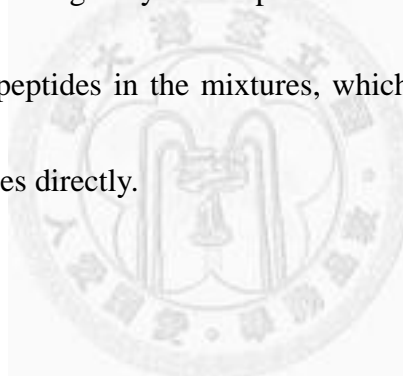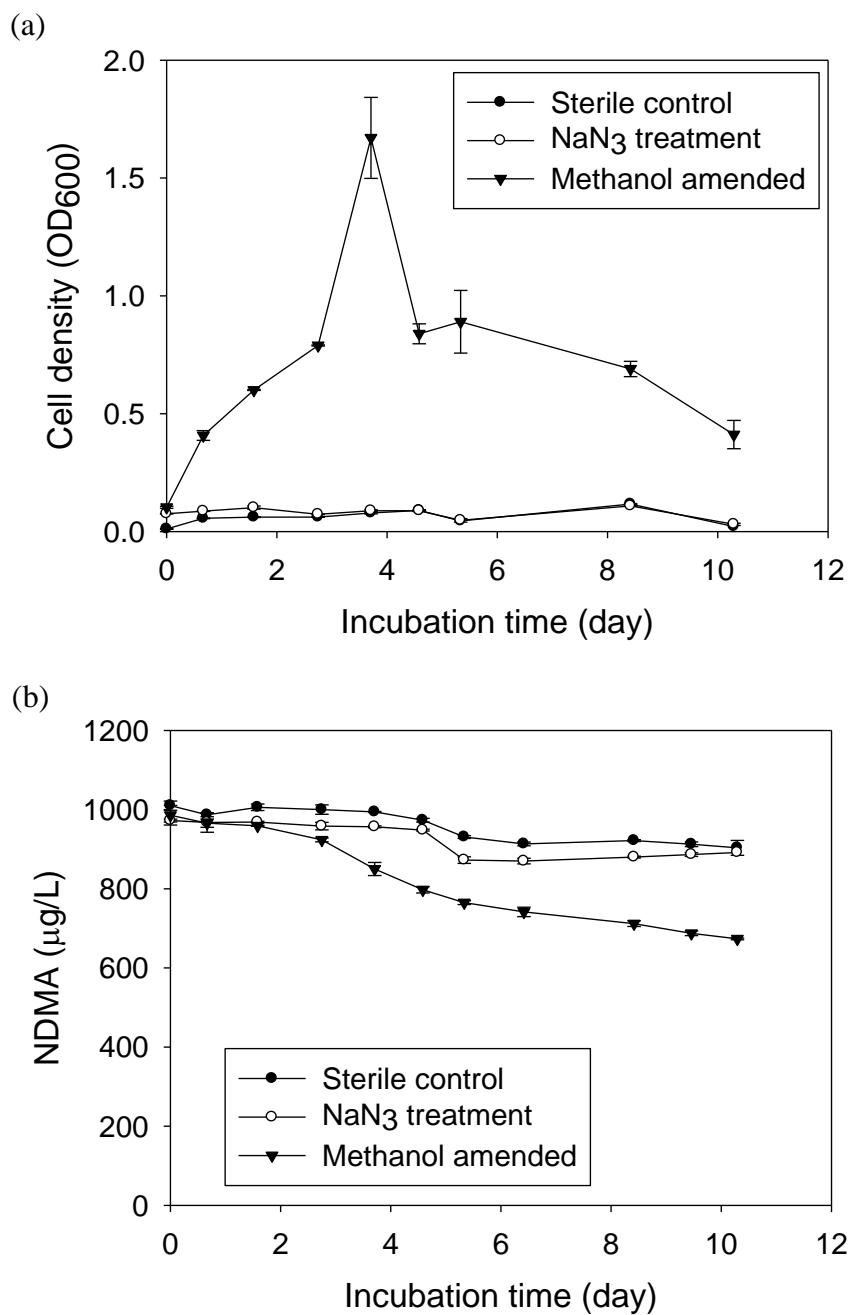
Figure 4. 4   NDMA bio-reduction by the isolate of *Methylobacterium* sp. in presence of methanol. (a) Cell density in N-BSM amended with methanol. (b) NDMA concentration during the incubation. Error bars represent the standard deviations of duplicate analysis.

(a)

(b)
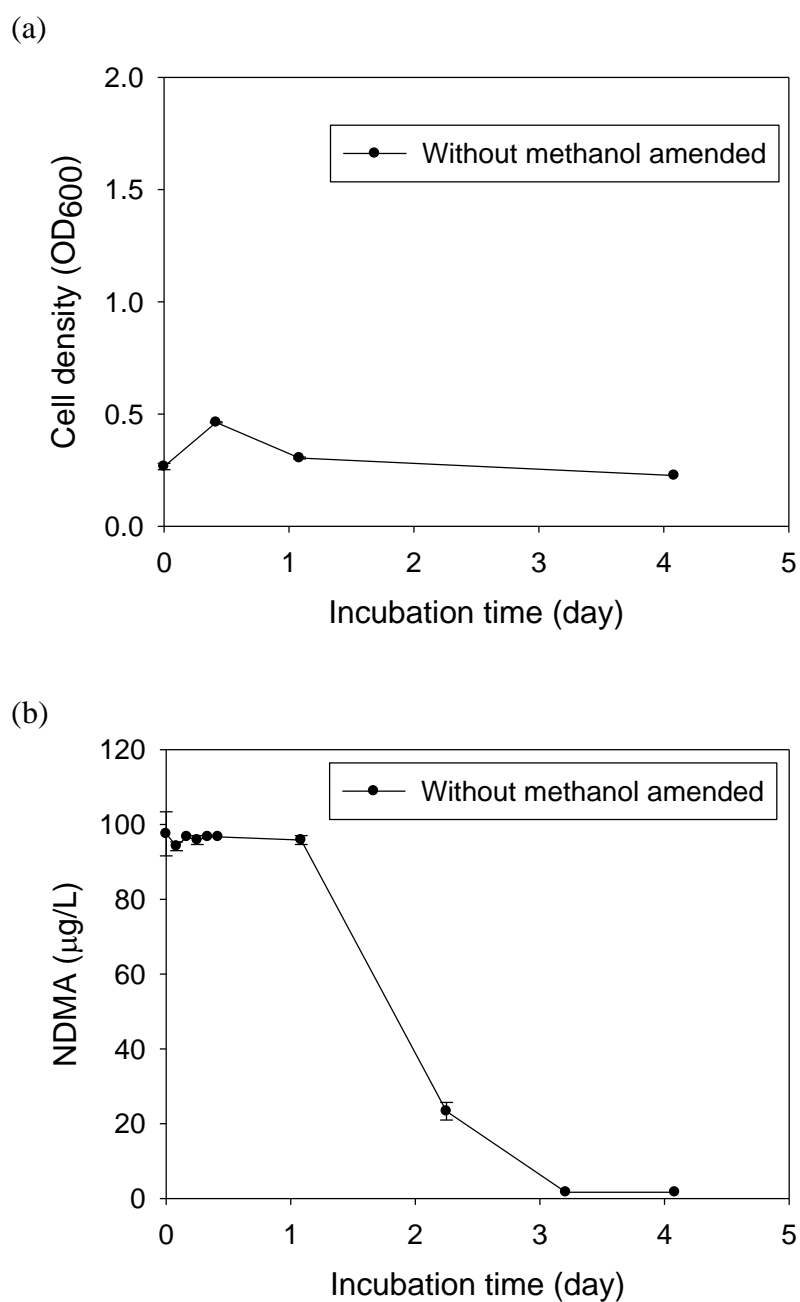
Figure 4. 5   NDMA bio-reduction by the isolate of *Methylobacterium* sp. in absence

of methanol. (a) Cell density in PBS. (b) NDMA concentration during the incubation.

Error bars represent the standard deviations of duplicate analysis.
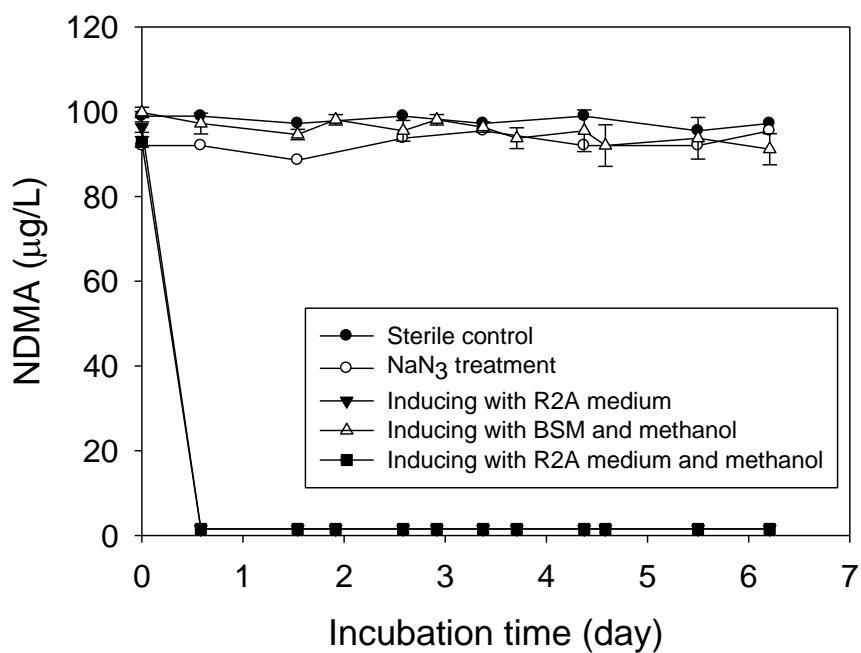
Figure 4. 6　Bio-reduction of NDMA by the isolate of *Methylobacterium* sp. after induced with different substrates. Error bars represent the standard deviations of duplicate experiments.

4.4   Kinetics of NDMA biotransformation by *Methylobacterium* sp.

In order to evaluate the factors affecting NDMA reduction by *Methylobacterium* sp., kinetic experiments associated with NDMA biotransformation were conducted in this section. As shown in Figure 4. 6, R2A medium was used as the substrates for pre-incubation with the bacterial isolate. R2A-grown cells were washed and suspended in N-BSM containing various concentrations of NDMA and the kinetic experiments were conducted at 15℃, 25℃, and 35℃, respectively.

The NDMA reduction curves showed that, at higher NDMA initial concentrations, more contact time was necessary to reach the 50% of NDMA removal by *Methylobacterium* sp.. For example, at 15℃, NDMA was half removed after 5 hours of contact time at the initial concentration of 50 μg/L NDMA; 10 hours of contact time at 100 μg/L NDMA; however, about 40 hours of contact time was needed to remove NDMA to the 50% as origin when initial concentration was 600 μg/L (Figure 4. 7). Similar results were observed when the experiments were conducted at 25℃ (Figure 4. 8), and less contact time was required to 50% of NDMA removal at 25℃ than 15℃. These results demonstrated that higher efficiency of NDMA biotransformation was happened at lower initial concentration and at 25℃. This did not mean that higher temperature resulted in greater performance on NDMA bio-reduction, otherwise, there was a different trend when the kinetic experiments were conducted at 35℃ (Figure 4. 9).

The reaction curves showed that the NDMA reduction was ceased after 23 hours of incubation over distinct NDMA initial concentrations at 35℃, and the proportion of reduction was about 50%. This phenomenon revealed higher temperature did not favor the NDMA biotransformation for the isolate.
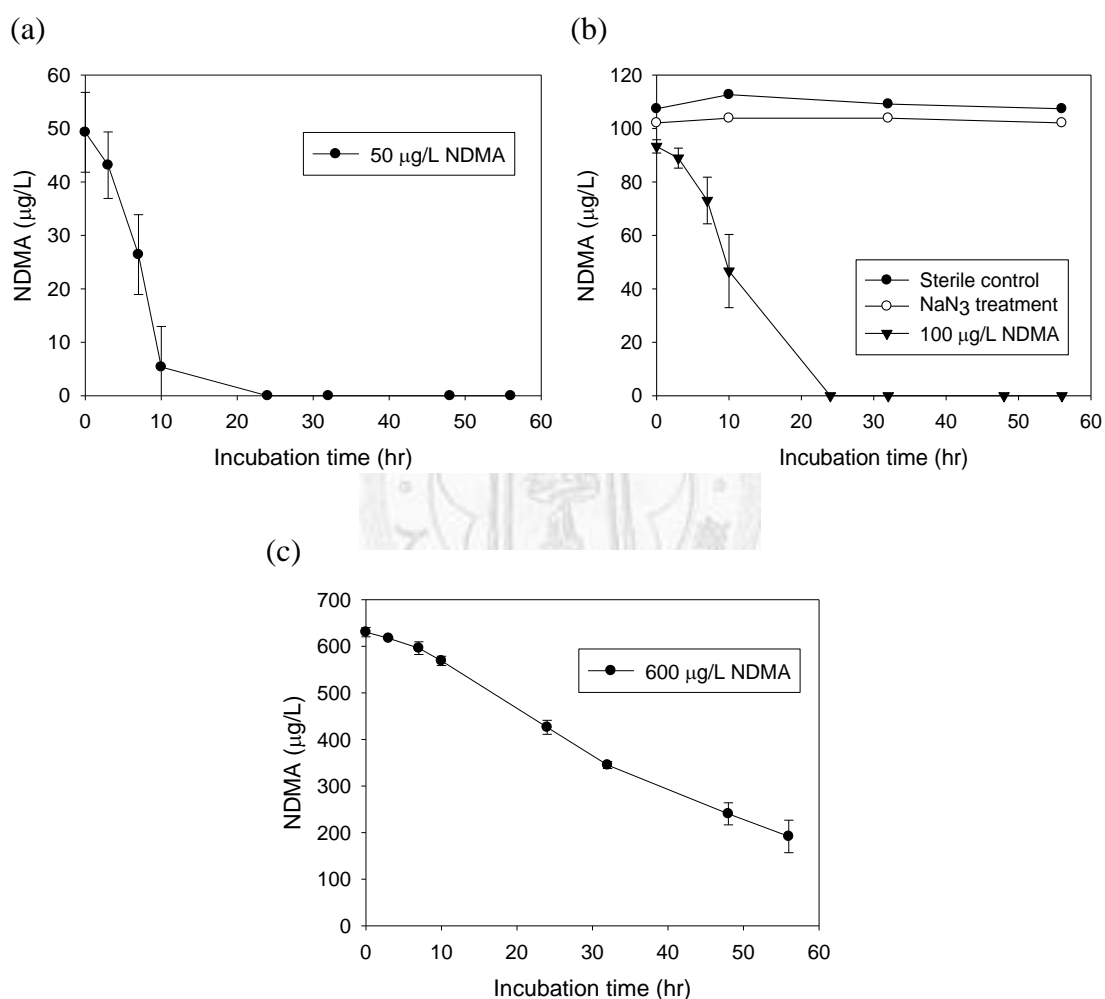
Figure 4. 7 NDMA reduction from various initial concentrations at 15℃ by the isolate of *Methylobacterium* sp.. (a) 50 μg/L; (b) 100 μg/L; (c) 600 μg/L. Error bars represent the standard deviations of duplicate experiments.
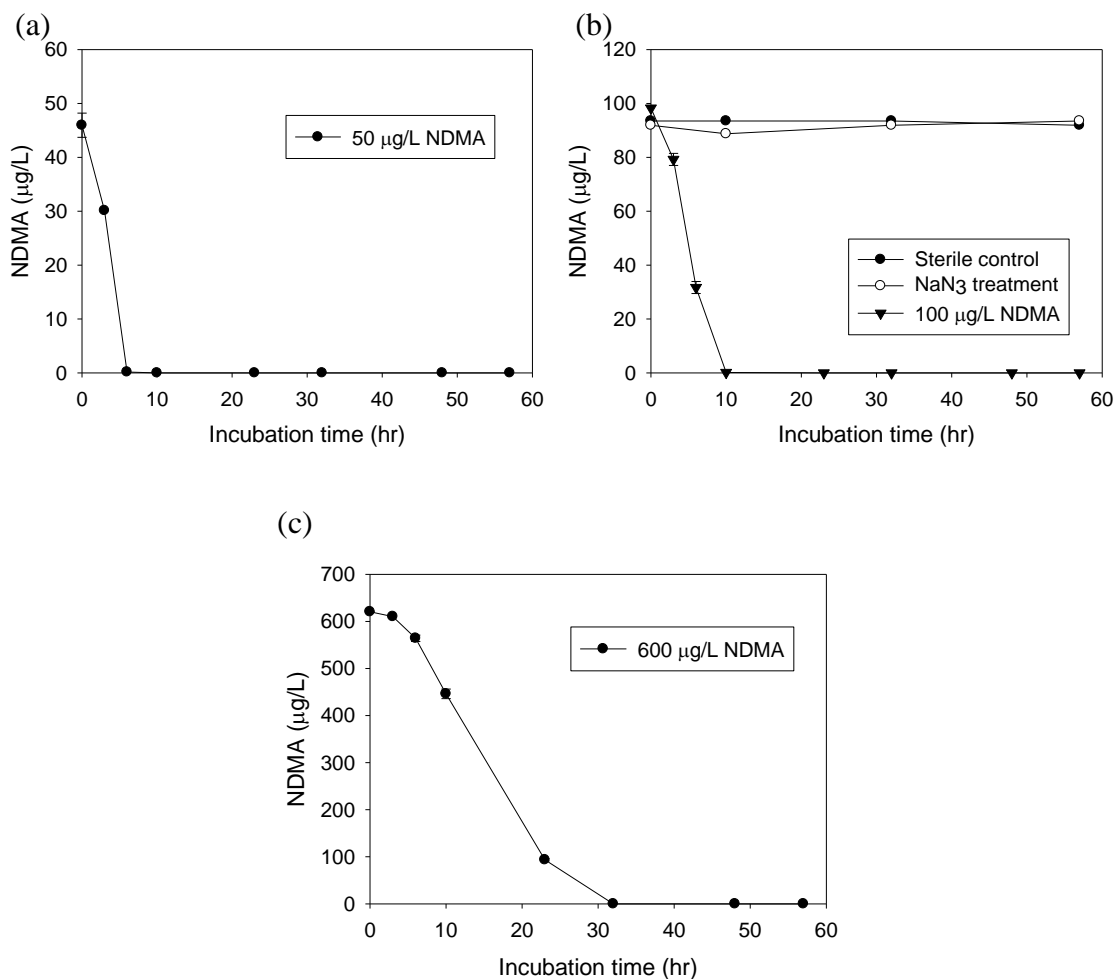
Figure 4. 8   NDMA reduction from various initial concentrations at 25℃ by the isolate of *Methylobacterium* sp.. (a) 50 μg/L; (b) 100 μg/L; (c) 600 μg/L. Error bars represent the standard deviations of duplicate experiments.

(a)

(b)

(c)
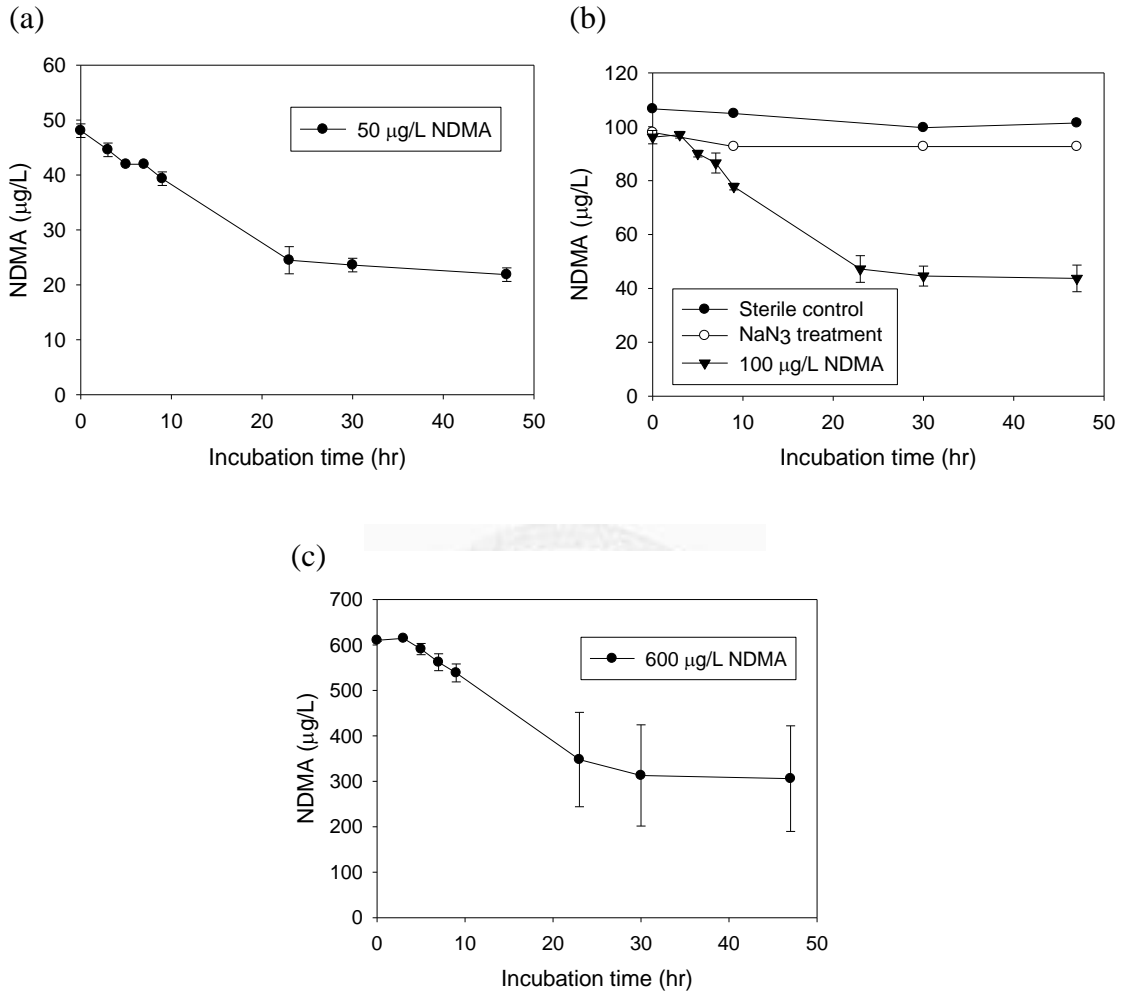
Figure 4. 9   NDMA reduction from various initial concentrations at 35℃ by the isolate of *Methylobacterium* sp.. (a) 50 μg/L; (b) 100 μg/L; (c) 600 μg/L; (d) semi-logarithmic plot as a function of time. Error bars represent the standard deviations of duplicate experiments.

First (1) and second (2) order kinetic model were fitted with the NDMA bio-reduction reaction, independently. The reduction curves could be linearized by transforming the NDMA concentrations into logarithmic (1) or reciprocal (2) scales, and the slope correlated with time depicted the rate constant of the reactions [107]:

$$\ln \frac{[C_t]}{[C_0]} = -k\mathrm{t} \qquad (1)$$

$$\frac{1}{[C_t]} = \frac{1}{[C_0]} + k\mathrm{t} \qquad (2)$$

where C_t is the NDMA concentration at a given time t, and C_0 denotes the initial NDMA concentration. The k value represents the reaction rate constant (hour^{-1}, in this study). The exact rate constants were determined based on the linear portion of the first order or second order transformation plots.

Compared to the results fitted with first (Figure 4. 10) and second (Figure 4. 11) order models, both of them provided better fits for kinetic data at higher initial concentrations, and this might attribute to the insufficient data points at lower concentrations. Overall, the fits of transformed NDMA concentrations with time were better by second order kinetic model than first order. It was observed that the rate constant was decreased when the initial concentration of NDMA was increased from 50 μg/L to 600 μg/L at 15℃ and 25℃ from both kinetic models, but their differences were not apparent when the system temperature was set at 35℃. It is possible that initial concentration was not an important factor affecting NDMA reduction at higher

77

temperature.

Figure 4. 12 shows a diagram, which was depicted with reaction rate (μg/L/hr) from each data point obtained in NDMA reduction curves as a function of time. The enzyme's maximum rate, V_{max}, was determined by the maximum value of regression curves. The results revealed that highest V_{max} was achieved at 25℃, about 30 μg/L/hr, and the lowest was observed at 15℃, about 9.4 μg/L/hr. The V_{max} at 35℃ was higher than 15℃, but it might be underestimated because the maximum rates were not indeed reached. As the results, enzymes become saturated with 400 μg/L of NDMA at 15℃, 350 μg/L of NDMA at 25℃, and more than 600 μg/L of NDMA at 35℃.
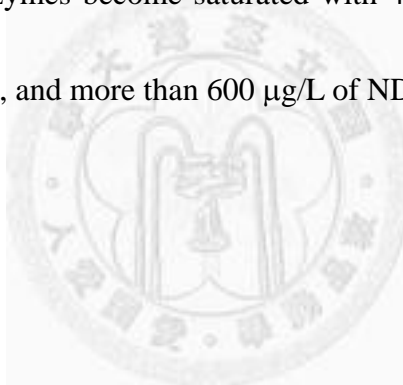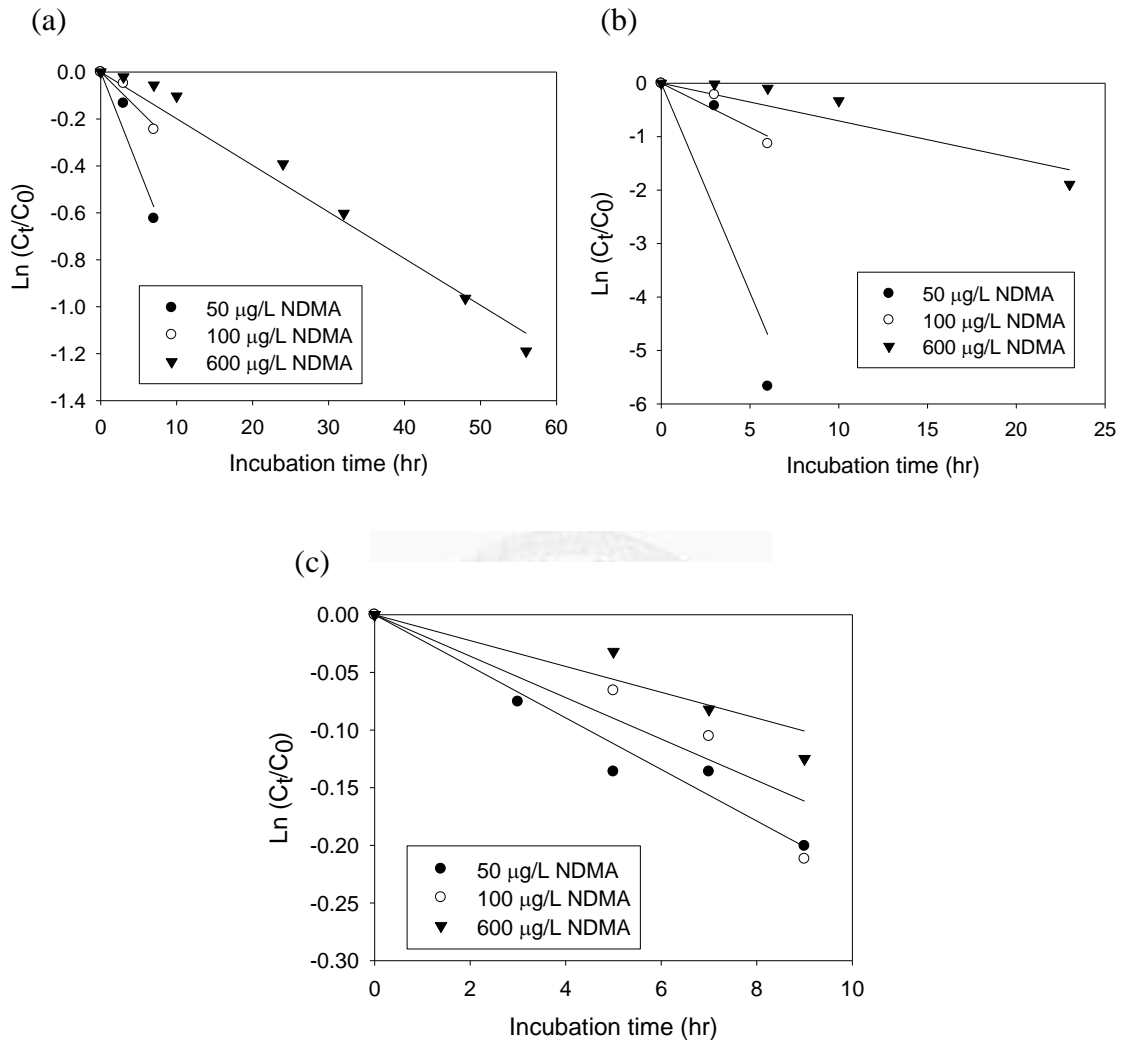
Figure 4. 10　　Semi-logarithmic transformation of NDMA concentrations as a function

of time according to first order reaction at various temperatures. (a) 15℃; (b) 25℃; (c)

35℃.
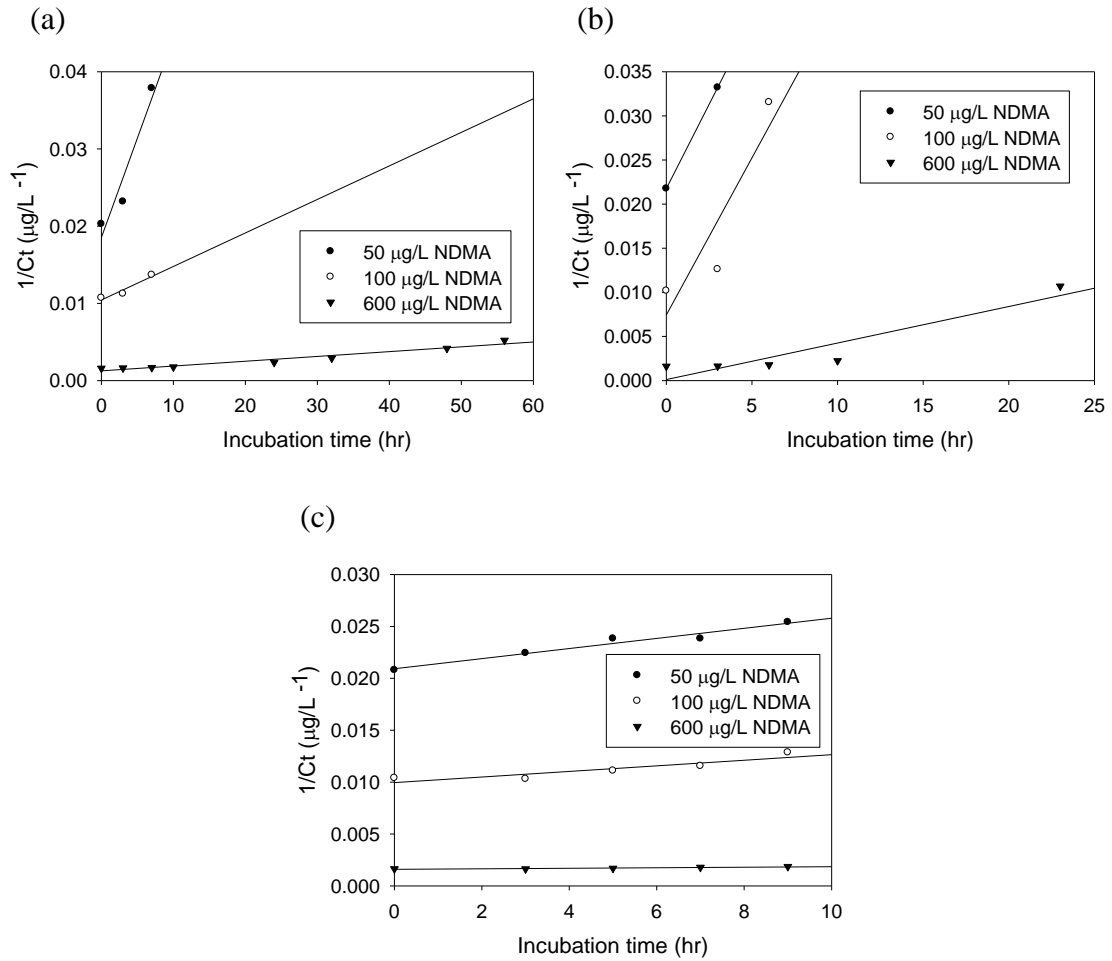
Figure 4. 11 Reciprocal transformation of NDMA concentrations as a function of time according to second order reaction at various temperatures. (a) 15℃; (b) 25℃; (c) 35℃.
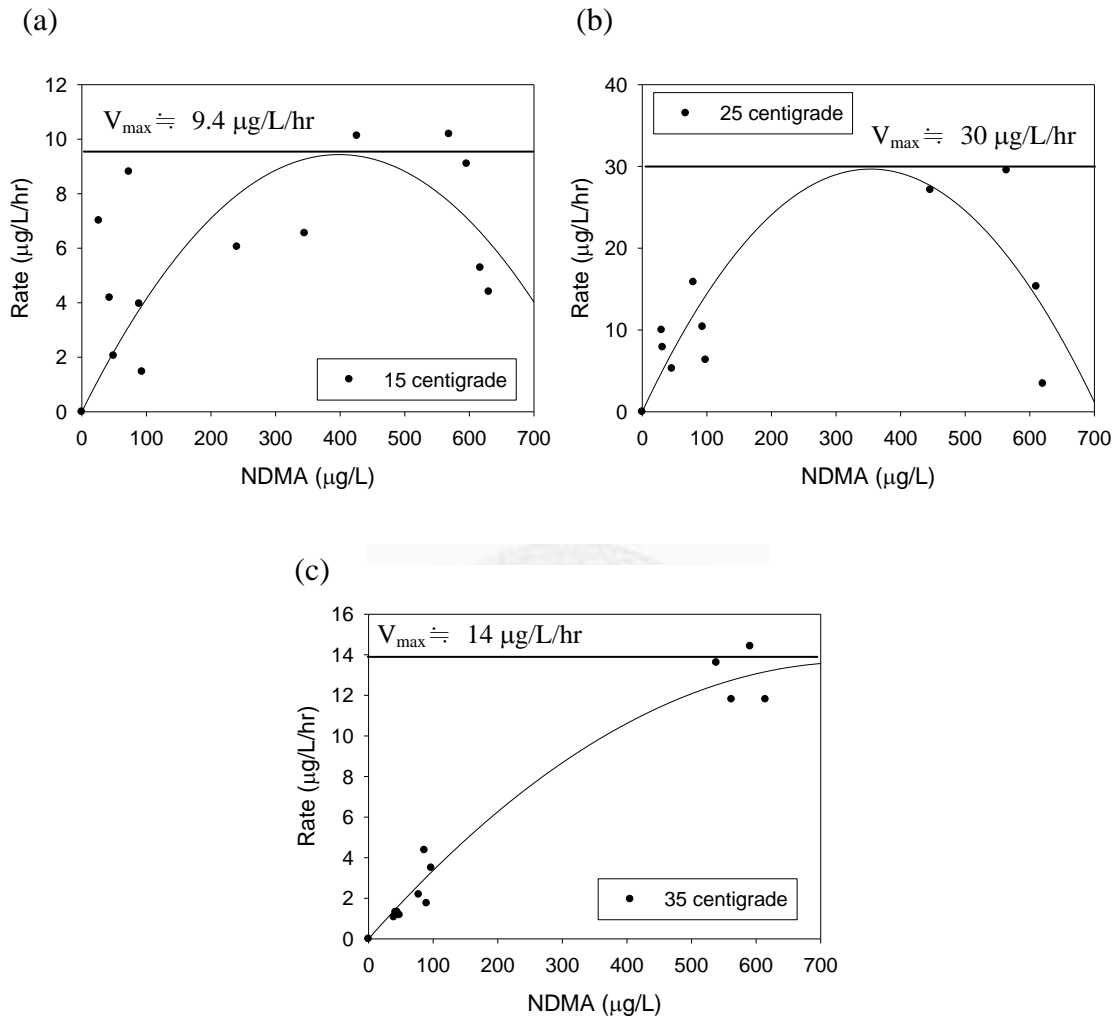
Figure 4. 12   Rate of NDMA reduction with different initial NDMA concentrations by the isolate of *Methylobacterium* sp. (a) 15℃; (b) 25℃; (c) 35℃. V_{max} was determined by the maximum value of the regression curve.

Table 4. 3 summarizes the results of the effects about temperatures and initial NDMA concentrations on the kinetics of NDMA biotransformation. Initial rates of NDMA reduction (μg/mg protein/hour) were calculated by the mass of NDMA reduced in the time period of exponential degradation curve and were expressed as a function of protein density. In addition, to assess NDMA reduction efficiency at various temperatures and initial concentrations, NDMA percentage removal after 10 hours of contact time after various experiments was compared in the Table 4. 3.

It can be seen that the initial reduction rates were increased with the increasing initial NDMA concentrations at each reaction temperature. Combined to the results demonstrated in Figure 4. 12, maximum reaction rates were reached with 600 μg/L of NDMA at 15℃ and 25℃, but not at 35℃. As shown in the results of kinetic studies analyzed with first order or second order reaction models, increases of the NDMA initial concentrations resulted in the decreases of rate constants and NDMA percentage removal for the experiments conducted at various temperatures. By analysis of first order kinetics, there was a 3 fold decrease when the NDMA initial concentration was increased from 50 μg/L to 600 μg/L at 15℃, a 35 fold decrease at 25℃, and a 2 fold decrease at 35℃. However, by analysis of second order kinetics, there was a 43 fold decrease when the NDMA initial concentration was increased from 50 μg/L to 600 μg/L at 15℃, a 9 fold decrease at 25℃, and a 2 fold decrease at 35℃. Although the exact

values were quite different, the tendency which represented the effects of initial NDMA

concentrations was the same.

To take the temperature effects into considerations, for the cases with the same

initial NDMA concentrations, it was observed that the rate constants and NDMA

percentage removal was the highest when the test temperature was 25℃ and the lowest

when the temperature was 35℃. These results indicated that NDMA biotransformation

reaction can be happened at a wide temperature ranges. Based on the results obtained in

this study, it was suggested the optimal temperature was approximately at the room

temperature (~ 25℃). However, the boundary of the suitable temperature ranges for

biodegradation of NDMA should be further studied.

Combined the results shown in Table 4.3, NDMA bio-reduction was exhibited

preferentially at 25℃ and lower initial NDMA concentrations. Fortunately, these

"preferred" conditions for NDMA biodegradation were almost identical to what is

observed in the natural water environments, therefore it is inferred that the NDMA

bio-reduction was applicable in the natural environment.

Table 4. 3   Temperature effects and initial NDMA concentrations for NDMA bio-reduction

| Reaction temperature | Initial concentration | | Initial reduction rate[+] | Rate constant* (hour^{-1}) | | Percent removal | V_{max} |
	NDMA (μg/L)	Protein (mg/ml)	(μg/mg protein/hour)	First order	Second order	after 10 hours (± SD%)	(μg/L/hr)
15℃	50	0.022	0.15	0.0822	0.00257	87.80 (17.25)	
	100	0.020	0.14	0.0320	0.00043	50.18 (13.35)	9.4
	600	0.022	0.36	0.0199	0.00006	9.75 (3.01)	
25℃	50	0.021	0.37	0.7842	0.00382	100 (0)	
	100	0.023	0.49	0.1652	0.00356	99.84 (0)	30
	600	0.020	1.14	0.0270	0.00041	28.10 (1.50)	
35℃	50	0.019	0.05	0.0224	0.00049	18.12 (4.68)	
	100	0.019	0.11	0.0180	0.00027	19.08 (0.80)	14
	600	0.022	0.37	0.0112	0.00003	11.47(3.60)	

+ Initial reduction rates were calculated by the mass of NDMA reduced in the time period of exponential reaction curve and expressed as a function of protein density.

* Rate constants are reported as the slope of logarithmic (first order) and reciprocal (second order) transformed linear regression.

Previous experiments were conducted in the N-BSM, which contained minimal salts and trace elements. However, that was quite different from the components of influents in the full scale slow sand filter in Kinmen. To estimate the extent of which might affect the efficiency of NDMA bio-reduction, the sterile influents of slow sand filter were spiked into the N-BSM containing 100 μg/L of NDMA to provide different proportions of sterile influents to the bacterial isolate. Figure 4. 13 (a) shows that addition of 10% and 50% influents in the N-BSM resulted in similar reduction curves, and the NDMA was eliminated in 23 hours of contact time at 25℃. However, a slower reduction for NDMA was observed when the batch experiment was conducted in 100% influents (no N-BSM). The reduction curves were fitted with first (Figure 4. 13 (b)) and second (Figure 4. 13 (c)) order kinetic models, but both of the kinetic plots showed less fit with the regression curves. It is possible that longer lag time was occurred in the influent matrixes than in N-BSM.

As the influents were spiked in the N-BSM, all indicators of NDMA biodegradation activity, which include the initial reduction rate, rate constants and NDMA percent removal after 10 hours of contact time, were decreased significantly (Table 4. 3, Table 4. 4). This phenomenon was more apparent in the case of 100% influent solutions, where the bacterial isolate still exhibited apparent capability of NDMA degradation, but the NDMA percentage degradation after 10 hours of contact

time was only 5.4 % (Table 4. 4). These findings were consistent with the studies

reported by Kaplan and Kaplan [10], in which they suggested that the rate of NDMA

mineralization were reduced when supplemental carbon was available. Because the

sterile influent was containing about 5.4 mg/L of NPDOC, the isolate of

Methylobacterium sp. might favor other organic compounds than NDMA. Another

possible explanation for the slow reduction rate could be elucidated by the dilution

effects of N-BSM, which might contain important elements for bioactivity. Therefore,

these results indicated that the efficiency of NDMA bio-reduction was probably

diminished in the slow sand filter.
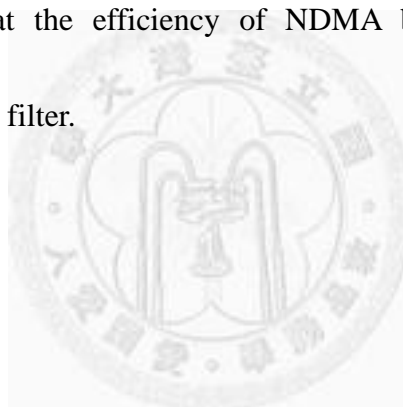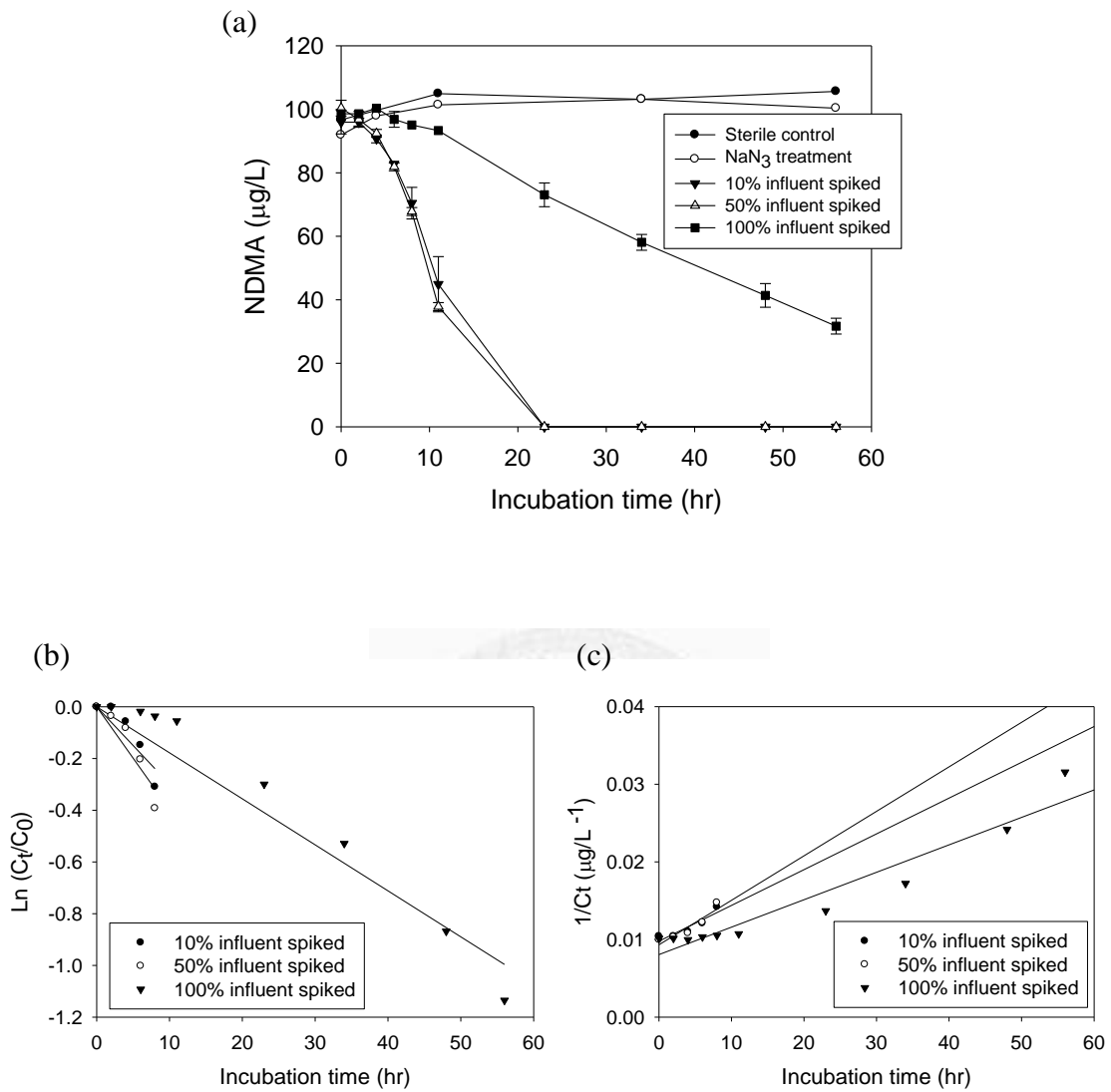
Figure 4. 13 The effects of influent substrates on NDMA reduction at 25℃ by the isolate of *Methylobacterium* sp.. (a) NDMA concentrations; (b) semi-logarithmic transformation according to first order reactions; (c) Reciprocal transformation according to second order reactions. Error bars represent the standard deviations of duplicate experiments.

Table 4. 4   The effects of field influents on NDMA bio-reduction at 25℃

| Influent spiked[#] | Initial concentration | | Initial reduction rate [+] | Rate constant* (hour^{-1}) | | Percent removal |
	NDMA (μg/L)	Protein (mg/ml)	(μg/mg protein/hour)	First order	Second order	after 10 hours (± SD%)
10%	100	0.017	0.18	0.0299	0.00046	53.35 (7.27)
50%	100	0.016	0.26	0.0397	0.00057	62.25 (2.18)
100%	100	0.014	0.08	0.0178	0.00035	5.36 (0)

# Sterile influents were spiked into nitrogen-containing BSM.

+ Initial reduction rates were calculated by the mass of NDMA reduced in the time period of exponential reaction curve and expressed as a function of protein density.

* Rate constants are reported as the slope of logarithmic (first order) and reciprocal (second order) transformed linear regression.

In order to elucidate the effects of mixed bacteria on NDMA bio-reduction, the other three bacterial isolates (as shown in section 4.1) were included in the batch kinetic experiments. At first, two kinds of mixed cultures were generated for kinetic study. First, the three bacterial isolates were inoculated separately and then amended with *Methylobacterium* sp. bacterial cultures for the kinetic study (referred as mixed cultures amended in Figure 4. 14 and Table 4. 5); second, the four bacterial isolates were inoculated together for subculture and then used for the kinetic study (referred as mixed subcultures in Figure 4. 14 and Table 4. 5). In the first mixed cultures, the cell quantity of *Methylobacterium* sp. was set at about half amount of the total cell numbers. Due to the slower growth of this *Methylobacterium* sp. isolate, however, the second mixed cultures contained only a small amount of *Methylobacterium* sp.. After that, the mixed cultures were used to perform NDMA reduction tests independently.

Compared to the pure bacterial culture of *Methylobacterium* sp., the first mixed cultures resulted in a similar NDMA reduction curve to the pure bacteria cultures, but no sustained NDMA reduction was found by the second mixed cultures where the bacteria were grown simultaneously (Figure 4. 14 (a)). Therefore, only reduction curves from pure cultures and mixed cultures amended were fitted by first and second order kinetic models (Figure 4. 14 (b) and (c)). Even though the slope of kinetic plots from mixed cultures amended was higher than that of pure bacterial cultures, but after

89

normalized to the cellular protein concentrations in the mixed cultures, the rate

constants by the reaction of mixed cultures were lower than that of pure bacterial

cultures (Table 4. 5). It is reasonable due to the cell quantity of *Methylobacterium* sp.

was less in mixed cultures than pure cultures. In addition, the percent removal of

NDMA after 10 hours of contact time showed that either pure bacterial culture (32.42%)

or the first mixed cultures (44.37%) performed higher NDMA bio-reduction efficiency

when compared to the second mixed cultures (17.22%).

In this experiment, two laboratory mixed cultures conditions were constructed. The

results suggested that *Methylobacterium* sp. was capable of NDMA bio-reduction under

these mixed bacteria conditions, but this ability might be restricted when the cell

numbers of other bacteria were much higher than the responsible bacterial isolate for

NDMA bio-reduction. Nevertheless, this could not be extended to the field mixed

bacteria conditions directly because the diversity and the abundance of microorganisms

consortia were complex and simulation in the laboratory might be different to field

conditions.
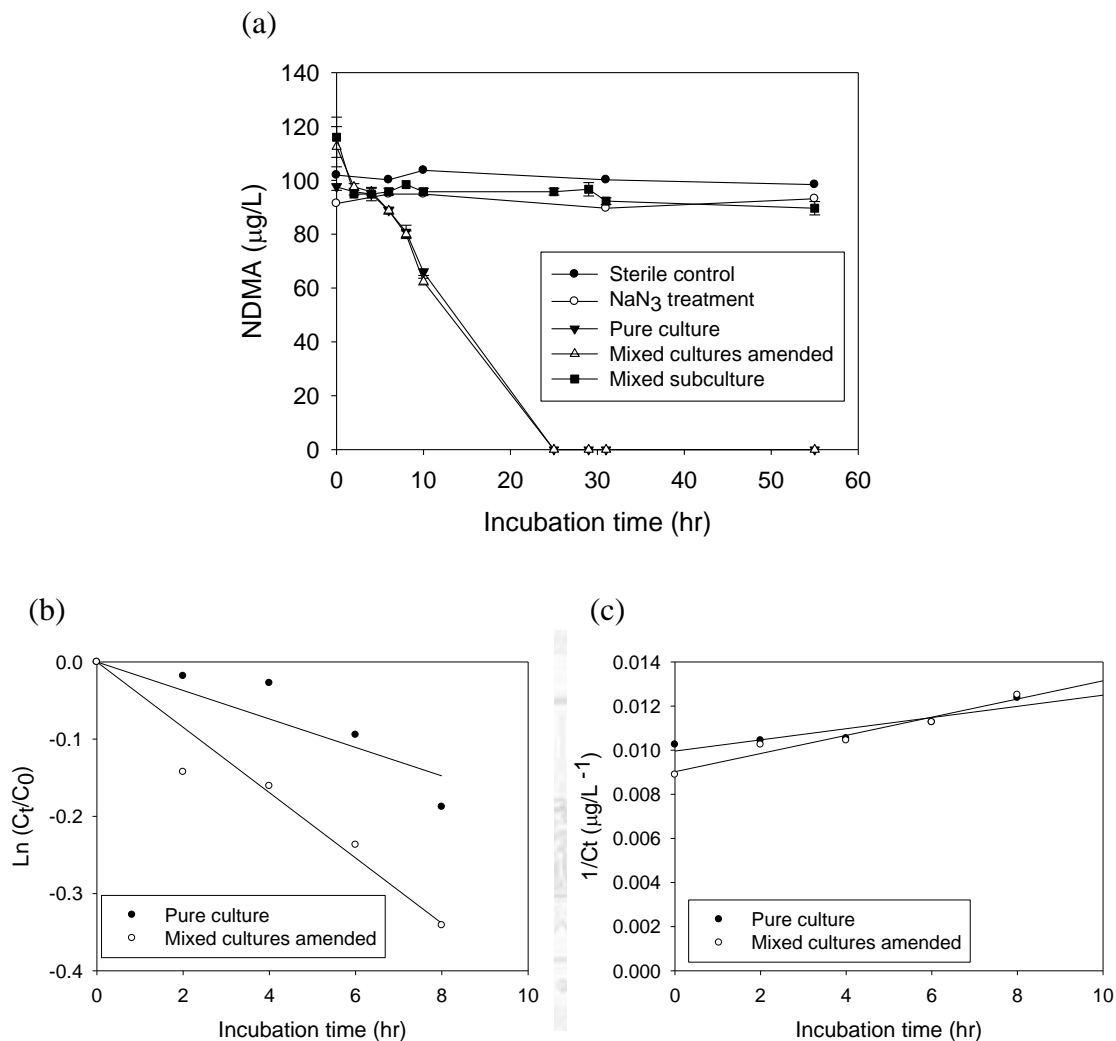
Figure 4. 14   The effects of mixed cultures on NDMA reduction at 25℃ by the isolate of *Methylobacterium* sp.. (a) NDMA concentrations; (b) semi-logarithmic transformation according to first order reactions; (c) Reciprocal transformation according to second order reactions. Error bars represent the standard deviations of duplicate experiments.

Table 4. 5　　The effects of mixed cultures on NDMA bio-reduction at 25℃

Cell cultures	Initial concentration		Initial reduction rate [+]	Rate constant* (hour^{-1})		Percent removal
	NDMA (μg/L)	Protein (mg/ml)	(μg/mg protein/hour)	First order	Second order	after 10 hours (± SD%)
Pure bacterial culture	100	0.018	0.12	0.0185	0.00025	32.42 (2.14)
Mixed cultures amended[#]	100	0.070	0.06	0.0109	0.00011	44.37 (4.79)
Mixed subculture[$]	100	0.057	0.04	---	---	17.22 (6.39)

Three bacterial isolates were inoculated separately and then amended with isolate of *Methylobacterium* sp. cultures followed by performing

NDMA reduction.

$ Four bacterial isolates were inoculated together and followed by performing NDMA reduction.

+ Initial reduction rates were calculated by the mass of NDMA reduced in the time period of exponential reaction curve and expressed as a

function of protein density.

* Rate constants are reported as the slope of logarithmic (first order) and reciprocal (second order) transformed linear regression and normalized

to the protein density.

4.5   Simulated column study

4.5.1   Bioactivity of acclimated microorganisms in the column

To investigate the NDMA-reducing bacteria on the different spatial scales of slow sand filter, a simulated sand column system with 1 m sand depth was installed in the laboratory. For acclimation of the microorganisms obtained from the field slow sand filter, the simulated sand column was fed with the influents from Kinmen water treatment plant's slow sand filter and spiked with 100 μg/L of NDMA.

Routine monitoring of NPDOC revealed that the effluent NPDOC concentrations were significantly reduced by 14% to 39% throughout the operating periods of the laboratory column system (Figure 4. 15 (a)). After 268 days of operation, influents and effluents of laboratory column were sampled for analysis of dissolved nitrogen species. The average concentration of total dissolved nitrogen in the influents was 1.26 mg/L, which was slightly higher than the concentration of total dissolved nitrogen in the effluents with 1.12 mg/L (Figure 4. 15 (b)). The measurement of inorganic nitrogen species showed that the average nitrate nitrogen increased from 0.17 mg/L to 0.39 mg/L, but a slightly decrease of 0.047 mg/L of ammonium nitrogen was observed. Besides, the changes of nitrite concentrations could be ignored since its concentration was very low. After subtracting the sum of inorganic nitrogen species from total dissolved nitrogen,

the average DON concentrations were 1.036 mg/L and 0.719 mg/L in the influents and effluents, respectively.

NPDOC concentrations in the WTP located in Kinmen were surveyed during November 2006 to May 2007 by our research group. According to the results, NPDOC concentrations were reduced by 3% to 26% after the slow sand filtration, which was slightly lower than the simulated sand column in this study (14% to 39%). Since NPDOC and DON may be the carbon and nitrogen sources of biofilm microbes on the sand surface, the reductions of NPDOC and DON concentration after the simulated sand column indicated that the biofilm remain active throughout the experiment. Moreover, the changes of ammonium and nitrate concentrations could be considered as the indicator of active microbial metabolic reactions.

(a)

(b)
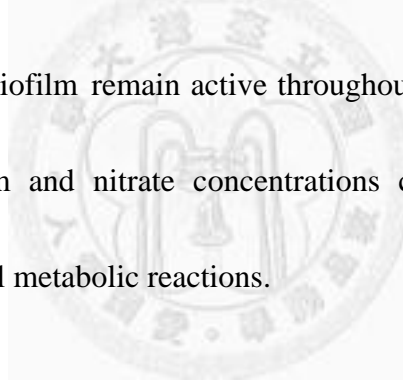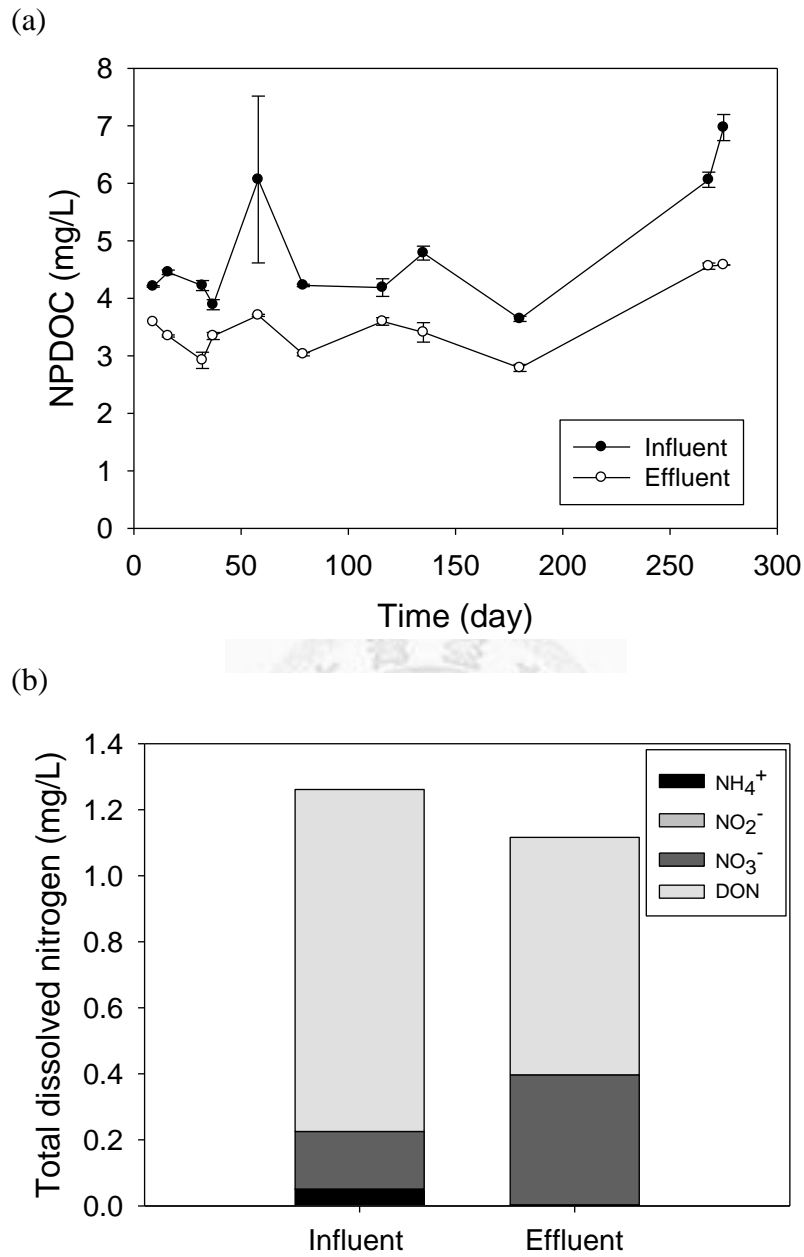
Figure 4. 15   Monitoring of NPDOC and dissolved nitrogen species through continuous column acclimation. Error bars in (a) represent the standard deviations of duplicate sampling and analysis. Values in (b) were obtained from the mean of sampling at two individual days.

4.5.2   Monitoring of NDMA concentrations through sand column system

The laboratory sand column was operated to evaluate its ability for NDMA removal under simulated field conditions. The average influent concentration of NDMA was 96.79 ± 6.19 μg/L, while the average effluent concentration of NDMA was 94.03 ± 5.53 μg/L throughout the operation period. There were no significant differences observed between influent and effluent concentrations of NDMA.

This consequence was similar to results reported by Nalinakumari *et al.* (2010), who established soil columns to investigate the effect of substrate concentration on NDMA biodegradation [62]. In their study, the soil columns were fed with drinking water that had a DOC concentration of about 3 mg/L, but negligible NDMA removal was observed. However, increasing the biodegradable DOC (BDOC) resulted in significant removal of NDMA. It seemed that a threshold of primary substrate concentrations should be reached to promote the cometabolic degradation of NDMA. There might be some critical factors in the field that we could not simulate in the laboratory column system. For example, schmutzdecke layer were not formed in the simulated sand column, so that organic substrates from photosynthetic activity could not be provided to the NDMA bio-reduction.

However, Nalinakumari *et al.* (2010) reported that mass removal rate was represented as 160 ng NDMA removed per mg DOC removed when the initial DOC

concentration was about 3.5 mg. In this study, NPDOC was removed by 0.5-2.4 mg/L

by the simulated sand column, therefore, it could be estimated that only 80 ng/L to 380

ng/L of NDMA was removed. This level was well below the detection limit (3.1 μg/L)

by analysis of HPLC coupled with diode array detector. Thus, it is still possible that

there were undetectable reductions of NDMA through the simulated sand column.
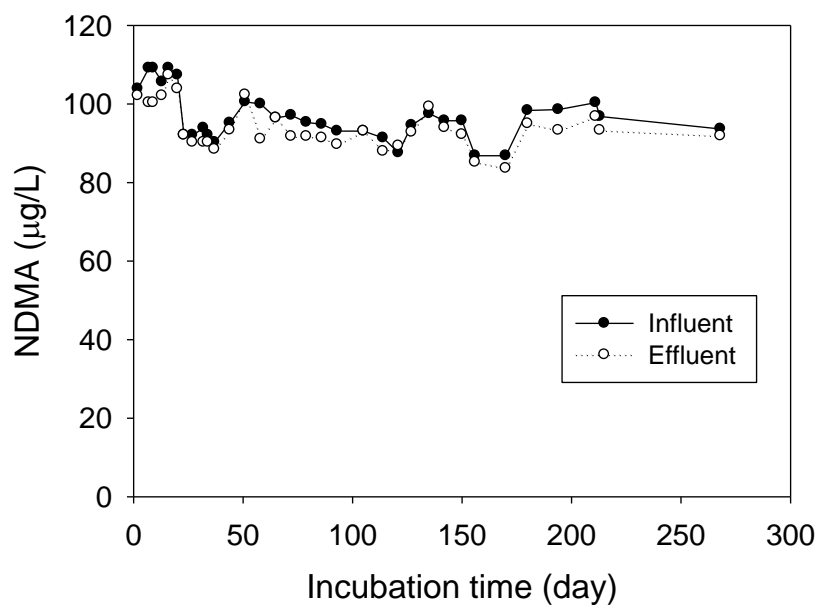
Figure 4. 16   Monitoring of NDMA concentrations through sand column system

4.6 Investigation of microbial community diversity and NDMA-reducing bacteria in the slow sand filter via T-RFLP method

T-RFLP is a sensitive method for rapid analysis of microbial community diversity in various environments [66, 70, 108]. In this section, we attempted to investigate the seasonal variations and spatial distribution of NDMA-reducing bacteria, and further compare the diversity among different microbial communities via T-RFLP.

4.6.1 Standard spectra construction of four bacterial isolates

From the spectra analysis demonstrated by T-RFLP, different peaks are corresponding to different DNA sequences of the cells, or referred to the phylotypes of microorganisms. However, the spectra analysis did not provide any information about what kind of species or strains the organisms were represented. Therefore, standard spectra of the specific bacterial isolates that we are interested in should be constructed for quantitative analysis. The practice of T-RFLP analysis to distinguish different phylogenetic bacterial isolates was evaluated by a CLC main workbench program simulation. The results revealed that those 16S rRNA gene sequences of four bacterial isolates, including *Sphingobium* sp. (Isolate A), *Terrabacter* sp. (Isolate B), *Methylobacterium* sp. (Isolate C) and *Bacillus* sp. (Isolate D), could produce distinguishable lengths of terminal restriction fragments (T-RFs) when double digested by restriction enzymes, *Xma*I and *Rsa*I.

Thus, the four bacterial isolates from the slow sand filter were initially used independently as the template for PCR amplification with 5' end fluorescently labeled universal oligonucleotide primers. After restriction enzyme digestion by *Xma*I and *Rsa*I, the intensity and exact lengths of T-RFs were determined using capillary gel electrophoresis coupled with a fluorescence detector. The standard spectra of four bacterial isolates were shown in Figure 4. 17, which revealed that the four peaks were distinguishable from each other. The spectra had excluded sizes less than 70 bp due to the interference of signals from residual primers. There were slight discrepancies between predicted lengths by computer simulation and observed lengths in reality. The predicted lengths for the T-RFs of the four bacterial isolates were 403, 144, 424, and 488 bp, respectively. However, the precise lengths obtained from the standard spectra were determined as 399, 141, 421, and 484 bp, respectively. According to the results of repeated analysis, the standard error was less than one base pair. This confirmed that the T-RFLP analysis was precise and reproducible for this study.
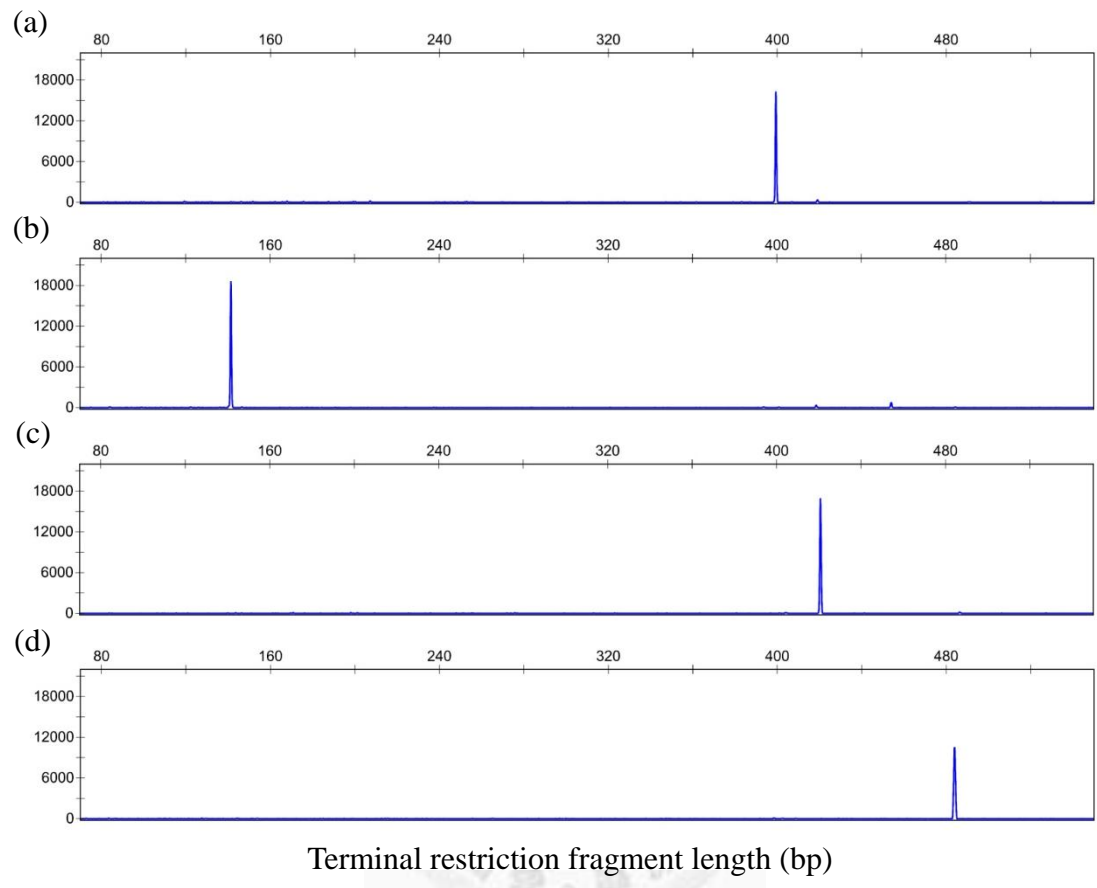
Figure 4. 17   Standard spectra of the bacterial isolates from slow sand filter. (a) Isolate

of *Sphingobium* sp. (Isolate A). (b) Isolate of *Terrabacter* sp. (Isolate B). (c) Isolate of

Methylobacterium sp. (Isolate C). (d) Isolate of *Bacillus* sp. (Isolate D).

4.6.2 Seasonal variation of microbial community diversity and distribution of the NDMA-reducing bacteria on the upper layer field slow sand filter

To demonstrate the existence and distribution of NDMA-reducing bacteria in the slow sand filter, the strategy of this study is to collect the sand samples from the upper layer of sand filter, which bleeds the most abundant microorganisms [16]. The total community DNA was isolated from the sand samples collected in summer and winter, respectively, and these DNA were then studied by T-RFLP analysis. The fragments between 75 and 550 bp corresponding to the size range of the standard were determined. The results showed that no distinguishable T-RFs larger than 525 bp were observed. The structure and diversity of the microbial community could be described by two parameters, species richness (numbers of species in a community) and species evenness (size of dominant species populations in a community).

The T-RFLP patterns for the sand samples taken in different seasons, summer and winter, revealed that the species diversities of the two communities were similar, but the relative species abundance were obviously different (Figure 4. 18). There were 57 and 61 distinct T-RFs in summer and winter sand samples observed, respectively. The abundant species were at the size range of 100 to 120 bp and the second was between 410 to 480 bp. However, the abundance of different species in summer was more evenly distributed than in winter. Based on the relative fluorescence intensity, the top five

species of the most abundant T-RFs accounted for 38.9% of the total microbial community (11.17, 10.9, 6.49, 5.59, 4.77%) in the summer, but 62.99% (17.55, 17.45, 11.29, 8.63, 8.07%) in winter (Table 4. 6). These results indicated that during the seasonal change, microbial species inhabited in the upper layer of slow sand filter was not changed significantly, but transitions from summer to winter might favor the survival of some dominant species.

T-RFs derived from NDMA-reducing bacterial isolates were also characterized (Table 4. 6). The isolate of *Methylobacterium* sp. accounted for only 0.63% of the total community in summer, but it was about doubled to 1.3% in winter. It might be due to lower temperature in winter more favorable for the survival of *Methylobacterium* sp. isolate than other species. These proportions of *Methylobacterium* sp. isolate in the slow sand filter might participate NDMA reduction from 11.4 ng/L to 3.7 ng/L and from 5.6 ng/L to below 3.2 ng/L in summer (May) and winter (January), respectively [15]. In addition, the other three bacterial isolates were mostly not detected by T-RFLP analysis, except a small amount (0.36%) of the isolate of *Bacillus* sp. (Isolate D) was observed in summer and the isolate of *Sphingobium* sp. (Isolate A) was observed in winter (0.57%) (Table 4. 6).
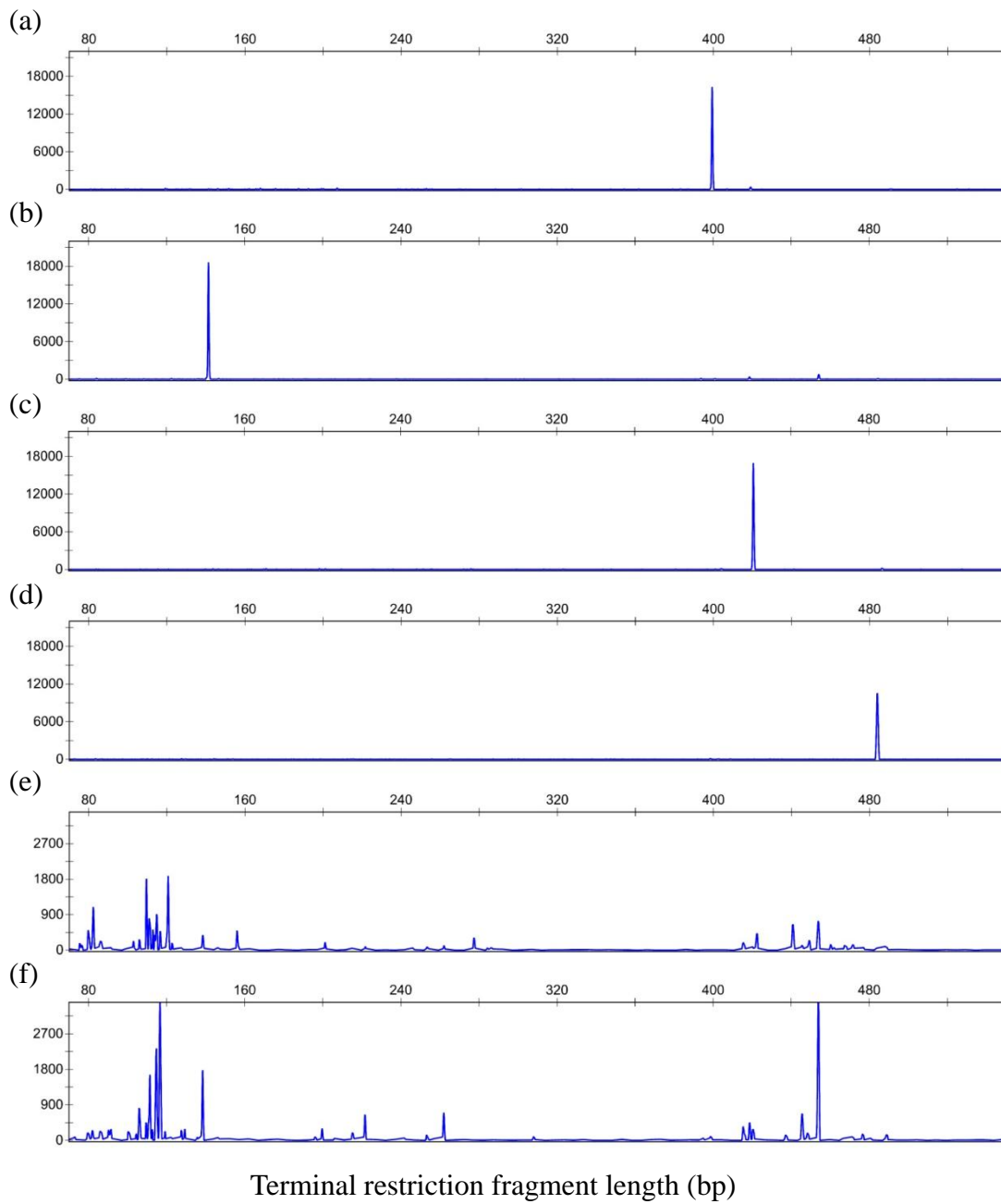
Figure 4. 18   Diversity of microbial community on the sand between seasonal changes.

(a) Isolate A. (b) Isolate B. (c) Isolate C. (d) Isolate D. (e) Summer sand. (f) Winter

sand.

4.6.3 Spatial variation of microbial community diversity and distribution of the NDMA-degrading bacteria in the simulated sand column

The simulated sand column system (section 4.5) provides an environment for natural formation of biological spatial levels. Four microbial layers were defined based on the column depths - upper layer (0 to 25 cm, Level I), upper-middle layer (25 to 50 cm, Level II), lower-middle layer (50 to 75 cm, Level III), and lower layer (75 to 100 cm, Level IV), respectively.

There were 16, 56, 35, and 27 distinct T-RFs existing in Level I to Level IV. In general, the species diversity was apparently lesser in the simulated sand column than those observed on sand samples taken from the field slow sand filter. Nevertheless, the species in Level II was more diverse than the other three layers (Figure 4. 19). When the species diversities in the four communities were compared, it was found that the abundance of T-RFs at the lengths between 75 and 100 bp was highly variable. Therefore, the phylogenetic species in this range might be possibly sensitive to the changes of nutrient or oxygen contents in the water flow through this region.

The isolate of *Methylobacterium* sp., which possessed the capability of NDMA bio-reduction, was only detected in Level II, and its relative quantity among the total microbial community was approximately 0.57%. The isolates of *Sphingobium* sp. (Isolate A) and *Terrabacter* sp. (Isolate B) were also detected in this layer with relative

quantity of 0.66% and 0.55%, respectively. In addition, the size range of T-RFs between 410 and 480 bp appeared in field sand samples was only present in Level II. Therefore, these results suggested that the diversity of microorganisms in Level II within the laboratory column was relatively similar to the microbial community in the upper layer of the field slow sand filter.

In this section, we had demonstrated that NDMA-reducing bacteria was detected in the simulated sand column system, but the structure of microbial community was significantly different when compared to that of the field slow sand filter, revealing the growth conditions in laboratory column were not similar to the situations in the field. Considering the relationships of biomass and ratio of NDMA concentration versus NPDOC, which is the primary source for microbial growth, there were largely differences between field conditions and experimental conditions. As the results shown by T-RFLP analysis, the proportion of *Methylobacterium* sp. was 0.63% in summer and 1.3% in winter, and 0.57% was containing in the Level II of sand column (Table 4. 6). According to the investigation of the WTP in Kinmen, 5-10 ng/L of NDMA [15] and about 5 mg/L of NPDOC were detected in the influents of slow sand filter, so that the ratio of NDMA/NPDOC was about 10^{-6}. Since the influents of simulated sand column were spiked with 100 μg/L of NDMA, the ratio of NDMA/NPDOC was increased about 4 orders. Therefore, it might be difficult to reduce high concentration of NDMA in the

sand column with almost similar biomass to the field. However, in the kinetic

experiments, various initial concentrations of NDMA from 50 µg/L to 600 µg/L were

significantly reduced by the *Methylobacterium* sp. isolate. This could be attributed to

the facts that much more biomass was brought into these experiments than the simulated

sand column.

Terminal restriction fragment length (bp)
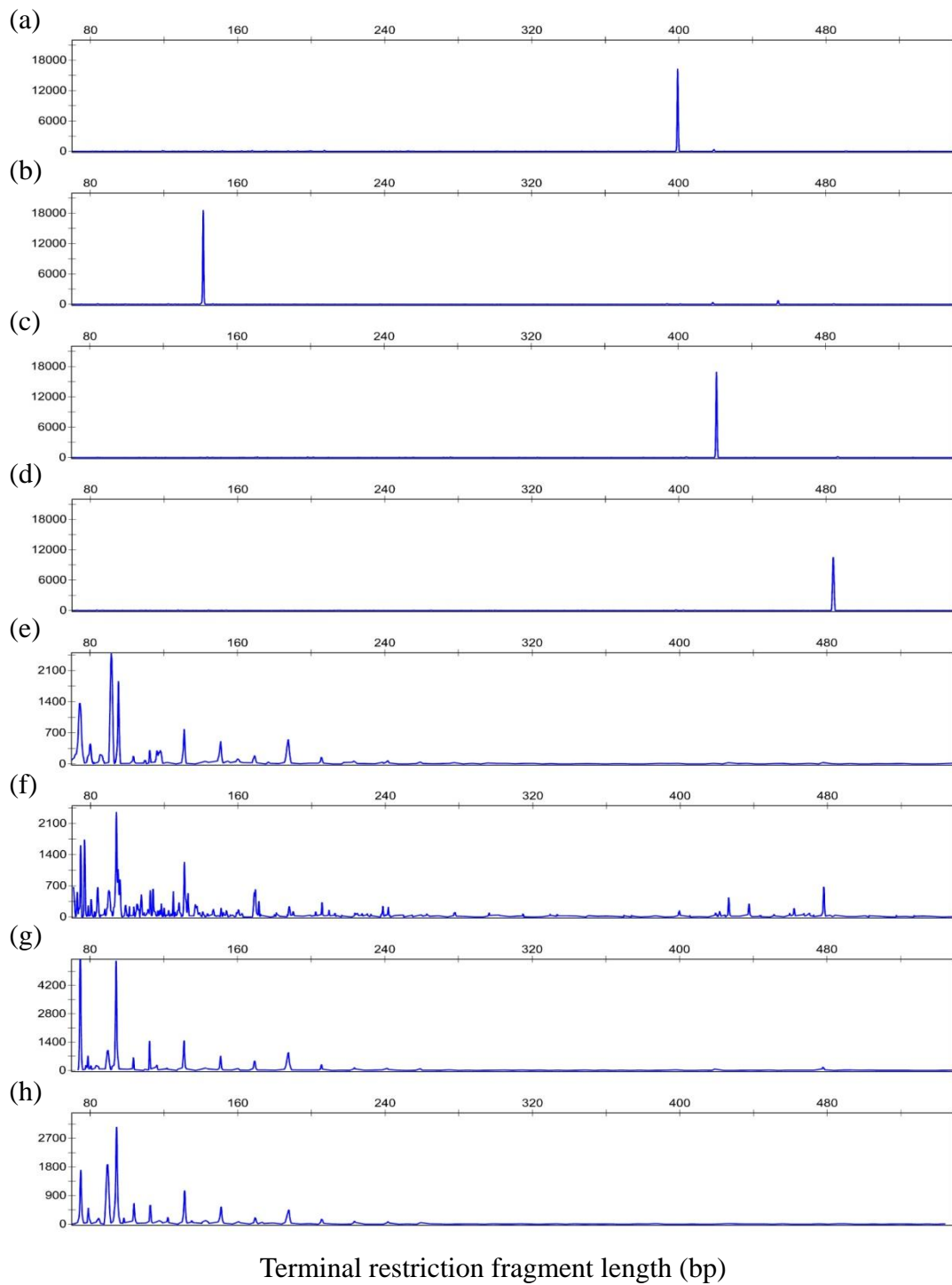
Figure 4. 19   Diversity of microbial community at different depths of simulated sand column. (a) Isolate A. (b) Isolate B. (c) Isolate C. (d) Isolate D. (e) Level I from upper layer (0 to 25 cm). (f) Level II from upper-middle layer (25 to 50 cm). (g) Level III from lower-middle layer (50 to 75 cm). (h) Level IV from lower layer (75 to 100 cm).

Table 4. 6   Relative abundance of microbial community in the slow sand filter and simulated sand column by T-RFLP targeting 16S rRNA gene sequences

Samples	Relative abundance (%)																
	75	77	78	79	80	82	84	85	86	88	89	90	91	92	94	95	96
Summer	1.3	0.99	---	---	3.15	6.49	---	---	1.57	---	---	0.3	0.58	---	---	---	---
Winter	---	0.21	0.27	---	0.91	1.16	---	---	1.03	---	---	1.24	1.24	---	---	---	---
Level I	13.46	---	---	---	4.48	---	---	---	2.41	---	---	---	---	24.4	---	18.32	---
Level II	7.01	7.53	---	1.13	1.73	0.55	2.9	---	---	0.79	---	2.64	---	---	10.26	4.64	3.67
Level III	25.33	---	1.35	3.21	1.14	---	1.3	---	---	---	---	4.48	---	1.02	23.84	---	---
Level IV	13.18	---	---	3.95	---	---	---	1.55	---	---	14.61	---	---	---	23.61	---	---
	98	99	100	101	103	104	105	106	107	110	111	112	113	114	115	116	117
Summer	---	0.31	---	---	1.53	0.3	---	1.82	---	10.9	4.77	---	3.12	2.35	5.59	---	3.06
Winter	---	---	1.07	---	---	0.75	---	3.53	---	1.92	6.86	---	1.16	---	9.6	---	14.93
Level I	---	---	---	---	---	1.79	---	---	---	---	---	3.07	---	---	---	3.07	2.71
Level II	---	1.28	---	1.04	1.01	---	1.35	---	2.2	---	0.87	2.61	---	2.72	0.63	0.73	0.67
Level III	---	0.5	---	0.4	---	2.83	---	---	---	0.45	---	6.41	---	0.46	0.81	1.24	0.41
Level IV	1.53	---	---	---	---	5.07	---	---	---	0.43	---	---	4.9	---	---	---	---

Table 4. 6　Relative abundance of microbial community in the slow sand filter and simulated sand column by T-RFLP targeting 16S rRNA gene sequences (continued)

Samples	Relative abundance (%)																
	118	119	120	121	122	123	125	126	128	129	131	133	135	136	137	138	B
Summer	---	---	---	11.17	---	1.37	---	---	0.48	---	---	---	---	---	---	2.39	---
Winter	---	1.02	---	---	0.71	---	0.24	---	1.23	1.18	---	---	---	0.39	0.38	7.34	---
Level I	3.07	---	---	---	---	---	---	---	---	---	7.72	---	---	---	---	---	---
Level II	1.3	---	0.89	---	0.69	---	2.5	0.47	1.41	---	5.39	2.33	---	---	1.24	1.07	0.55
Level III	---	---	---	---	0.83	---	---	---	0.58	0.51	6.47	---	0.48	---	---	---	0.43
Level IV	1.19	---	---	---	1.83	---	---	---	---	0.39	8.35	---	1.22	---	---	---	0.81
	143	144	147	151	154	155	156	159	160	161	162	163	165	166	169	170	171
Summer	---	---	0.62	---	---	---	2.94	---	---	---	---	0.47	---	0.42	---	---	---
Winter	---	0.21	0.47	---	---	---	---	---	---	---	0.59	---	0.34	0.3	---	---	---
Level I	---	---	---	4.98	---	---	---	---	1.4	---	---	---	---	---	2.03	---	---
Level II	---	---	0.76	0.88	0.64	---	---	0.47	0.71	---	---	---	---	---	2.67	---	1.56
Level III	0.68	---	0.4	3.17	---	---	---	---	---	0.5	---	---	---	---	2.29	---	---
Level IV	1.03	---	---	4.45	---	0.4	---	---	---	0.87	---	---	---	---	---	1.93	---

Table 4. 6   Relative abundance of microbial community in the slow sand filter and simulated sand column by T-RFLP targeting 16S rRNA gene sequences (continued)

Samples	Relative abundance (%)																
	174	175	183	188	190	196	200	201	202	206	209	215	222	224	230	239	242
Summer	---	---	---	---	---	---	---	1.35	---	---	---	0.51	0.72	---	---	---	---
Winter	---	0.26	0.21	---	---	0.56	1.31	---	---	0.26	---	0.96	2.79	---	0.22	---	0.4
Level I	---	---	---	5.56	---	---	---	---	---	1.55	---	---	---	---	---	---	---
Level II	---	---	---	1.13	0.66	---	---	---	0.6	1.42	0.69	---	---	0.49	---	1.13	0.98
Level III	---	---	---	4.06	---	---	---	---	---	1.31	---	---	---	0.68	---	---	0.7
Level IV	0.55	---	---	3.7	---	---	---	---	---	1.56	---	---	---	0.99	---	---	0.86
	246	249	253	254	257	260	262	277	278	284	286	292	293	308	395	A	400
Summer	0.45	---	---	0.78	---	---	0.83	2.01	---	0.46	0.44	0.36	0.36	---	---	---	---
Winter	---	0.22	0.74	---	0.26	---	2.88	---	---	---	---	---	---	0.5	0.31	0.57	---
Level I	---	---	---	---	---	---	---	---	---	---	---	---	---	---	---	---	---
Level II	---	---	---	---	---	---	---	---	0.53	---	---	---	---	---	---	---	0.66
Level III	---	---	---	---	---	0.38	---	---	---	---	---	---	---	---	---	---	---
Level IV	---	---	---	---	---	0.66	---	---	0.38	---	---	---	---	---	---	---	---

Table 4. 6   Relative abundance of microbial community in the slow sand filter and simulated sand column by T-RFLP targeting 16S rRNA gene sequences (continued)

Samples	Relative abundance (%)																
	415	419	C	422	426	433	437	438	441	446	448	449	454	460	462	467	468
Summer	1.27	0.46	0.63	2.77	---	---	0.33	0.43	4.07	0.93	---	1.62	4.53	0.94	0.47	0.94	0.85
Winter	1.46	1.95	1.3	---	---	0.21	0.62	---	---	2.93	0.91	---	14.85	---	---	0.52	---
Level I	---	---	---	---	---	---	---	---	---	---	---	---	---	---	---	---	---
Level II	---	0.52	0.57	---	1.88	---	1.28	---	---	---	---	---	---	---	0.92	---	---
Level III	---	0.44	---	---	---	---	---	---	---	---	---	---	---	---	---	---	---
Level IV	---	---	---	---	---	---	---	---	---	---	---	---	---	---	---	---	---

	472	477	478	481	482	D	488	489
Summer	0.9	0.5	---	0.72	0.3	0.36	0.69	---
Winter	0.44	0.8	---	0.62	---	---	---	0.66
Level I	---	---	---	---	---	---	---	---
Level II	---	---	2.98	---	---	---	---	---
Level III	---	---	0.91	---	---	---	---	---
Level IV	---	---	---	---	---	---	---	---

Chapter V   Conclusions and recommendations

5.1   Conclusions

To evaluate the potential of NDMA reduction by the biofitration in drinking water treatment plant, this study use a low-nutrient medium, R2A, to isolate oligotrophic bacteria from slow sand filter. Four bacterial isolates obtained from the R2A incubations were tested, and only the isolate of *Methylobacterium* sp. exhibited apparent ability of NDMA reduction. This bacterial isolate was reported as a pink-pigmented facultative methylotrophic (PPFM) bacterium, which was widely found from various environments, also in the chlorine-containing drinking water system.

The metabolic characteristics on the isolate of *Methylobacterium* sp. demonstrated that the bacterial isolate performed NDMA bio-reduction not by utilizing NDMA as the carbon energy source and/or nitrogen source, but via the cometabolism mechanism after growth in the presence of R2A medium.

The results of kinetic experiments showed that many factors affecting NDMA biotransformation by the *Methylobacterium* sp. isolate. NDMA was reduced over the initial concentrations of 50 μg/L to 600 μg/L and higher NDMA initial concentrations need longer contact time to remove half amounts of NDMA. The rate constant ($hour^{-1}$) decreased when the initial concentration of NDMA was increased at various

temperatures (15℃ and 25℃) from both first and second order kinetic models, but their differences were not apparent when the system temperature was set at 35℃. In addition, V_{max} was the highest at 25℃, about 30 μg/L/hr; and the lowest was at 15℃, about 9.4 μg/L/hr. The V_{max} at 35℃ was higher than 15℃, but it might be underestimated because the maximum rates were not indeed reached. These results indicated that NDMA biotransformation can occurred at a wide temperature ranges, but the optimal temperature was approximately at room temperature.

After spiking different proportions of sterile influents from field slow sand filter, slower reduction rate was observed when the batch experiment was conducted in 100% of field influent. This result indicated that the isolate of *Methylobacterium* sp. might favor other organic compounds than NDMA or there were insufficient mineral salts in the influents of slow sand filter for the NDMA bio-reduction. In addition, the isolate of *Methylobacterium* sp. could possess NDMA bio-reduction ability under simulated mixed bacteria conditions as well, but this ability might be restricted when the cell numbers of other bacteria were much higher than the responsible bacterial isolate.

T-RFLP analysis is a precise and reproducible technique for rapid analysis and comparison of microbial communities. T-RF derived from the isolate of *Methylobacterium* sp. accounted for only 0.63% of the total community for sand samples taken in summer, and about twice in winter (1.3%).

In the simulated sand column, which provided an environment for natural formation of biological spatial layers, no significant NDMA removal was observed even though NPDOC and DON were reduced. The four microbial communities defined according to the column depths were compared via T-RFLP analysis, and the T-RF patterns revealed that the diversity of microorganisms in the upper-middle layer (25 to 50 cm, Level II) was relatively similar to the microbial community in the upper layer of field slow sand filter. Also, the isolate of *Methylobacterium* sp. was only detected in Level II, and the relative quantity was 0.57% of total community.

In summary, the results in this study showed that the NDMA bio-reduction during slow sand filter in the drinking water treatment plant is possible due to the presence of NDMA-reducing bacteria. However, the effects from organic and inorganic substrates, mixed bacteria and the optimal operation conditions should also be considered.

5.2   Recommendations

- In this study, we had focused on the characterization of the isolate of *Methylobacterium* sp., but there were probably other bacteria which have ability to reduce NDMA in the slow sand filter. For fully evaluation on the potential of NDMA removal in slow sand filter, more bacteria should be isolated and assessed their relationships between different NDMA-reducing bacteria.

- We had demonstrated the capability of NDMA biotransformation by the *Methylobacterium* sp. isolated from the slow sand filter, but apart from the real situations in the field, suspended cultivations were used for the batch experiments in this study. For future studies, the isolate of *Methylobacterium* sp. containing biofilm attached on the sand could be used as the biological materials for the kinetic experiments.

- In this study, cometabolism was assumed as the major approach for NDMA biotransformation by the *Methylobacterium* sp. isolate. However, monooxygenase activity should be tested on the *Methylobacterium* sp. isolate for more confirmation. In addition, several hydrocarbons, such as methane, propane, and toluene, were proved as the inducing substrate for NDMA biodegradation. In this study, we found that R2A served as the inducing substrates to activate enzymes responsible for NDMA bio-reduction. However, due to the complex compositions in the R2A

medium, we could not elucidate which one is the primary substrate participating NDMA cometabolic biotransformation. Among the organic substances in R2A medium, amino acids were the most possible substrates to induce expression of cometabolic enzymes. Therefore, for future studies, different amino acids and the reported hydrocarbons should be further tested.

- Although it was not observed that NDMA was significantly removed by simulated sand column, there were several possibilities for explanation. First, based on the estimated mass removal rate by Nalinakumari et al. (2010), the reduced level of NDMA was well below the detection limit (3.1 µg/L) by HPLC coupled with diode array detector, so that a more sensitive method for NDMA analysis should be used. Second, since the ratio of NDMA/NPDOC of simulated sand column was increased about 4 orders than the field slow sand filter, it might be difficult to reduce such higher concentration of NDMA in the sand column with almost similar biomass to the field. To improve the designs on simulated column study, concentrations of NPDOC and NDMA in the influents should be adjusted to the same ratio as field conditions.

- T-RFLP is a powerful technique for analysis of community diversity at various environmental conditions and distinct organisms. In this study, T-RFLP patterns represented the possible distributions of NDMA-reducing bacteria in different sand

communities. The results found that the isolate of *Methylobacterium* sp. was present at a relatively small proportion of the total community in the upper layer slow sand filter. However, the exact quantities of the target bacteria in the field were unclear. For the future studies, quantitative real-time PCR could be used for detection and quantification of the bacterial isolate, even when they are existed in a much lower cell numbers. Therefore, the two methods should be conducted simultaneously to provide more information regarding to the NDMA-reducing bacteria in the slow sand filter.

References

1. ATSDR, *Toxicological profile for N-nitrosodimethylamine*. 1989.

2. USEPA, *Integrated Risk Information System (IRIS). N-Nitrosodimethylamine (CASRN 62-75-9)*. 2006.

3. WHO, *Concise international chemical assessment document (CICAD) 38, N-nitrosodimethylamine*. 2002.

4. SFPUC, *San francisco public utilities commission. N-nitrosodimethylamine (NDMA) information*. 2007.

5. Mitch, W.A., et al., *N-Nitrosodimethylamine (NDMA) as a drinking water contaminant: A review.* Environmental Engineering Science, 2003. **20**(5): p. 389-404.

6. CDHS, *California department of health service. Studies on the occurrence of NDMA in drinking water*. 2002.

7. WHO, *N-nitrosodimethylamine in drinking water. Background document for development of WHO guidelines for drinking-water quality*. 2008.

8. Mitch, W.A. and D.L. Sedlak, *Formation of N-nitrosodimethylamine (NDMA) from dimethylamine during chlorination.* Environmental Science & Technology, 2002. **36**(4): p. 588-595.

9. Stefan, M.I. and J.R. Bolton, *UV direct photolysis of N-nitrosodimethylamine (NDMA): Kinetic and product study.* Helvetica Chimica Acta, 2002. **85**(5): p. 1416-1426.

10. Kaplan, D.L. and A.M. Kaplan, *Biodegradation of N-Nitrosodimethylamine in Aqueous and Soil Systems.* Appl Environ Microbiol, 1985. **50**(4): p. 1077-1086.

11. Gunnison, D., et al., *Attenuation mechanisms of N-nitrosodimethylamine at an operating intercept and treat groundwater remediation system.* J Hazard Mater, 2000. **73**(2): p. 179-97.

12. Bradley, P.M., et al., *Biodegradation of N-nitrosodimethylamine in soil from a water reclamation facility.* Bioremediation Journal, 2005. **9**(2): p. 115-120.

13. Bombach, P., et al., *Current approaches for the assessment of in situ biodegradation.* Applied Microbiology and Biotechnology, 2010. **86**(3): p. 839-852.

14. Tate, R.L., 3rd and M. Alexander, *Stability of nitrosamines in samples of lake water, soil, and sewage.* J Natl Cancer Inst, 1975. **54**(2): p. 327-30.

15. Hung, S.W., et al., *Trace analysis of N-nitrosamines in water using solid-phase microextraction coupled with gas chromatograph–temdem mass spectrometry.* Water air and soil pollution, 2010.

16. Campos, L.C., et al., *Biomass development in slow sand filters.* Water Research, 2002. **36**(18): p. 4543-4551.

17. Najm, I. and R.R. Trussell, *NDMA formation in water and wastewater.* American Water Works Association Journal, 2001. **93**(2): p. 92-99.

18. USEPA, *Emerging contaminant - N-nitrosodimethylamine (NDMA).* 2008.

19. OEHHA. *Announcement of publication of the final public health goal for N-Nitrosodimethylamine and cadmium in drinking water accessed at:* http://oehha.ca.gov/water/phg/cadndma122206.html. 2006.

20. FDA, *Compliance policy guidelines (CPG) section 500.450. Volotile N-nitrosamines in rubber baby bottle nipples.* 2005.

21. OCWD, *Orange County Water District takes a proactive stance on newly regulated compound N-nitrosodimethylamine: OCWD recommends taking two drinking water wells out of serve.* 2000.

22. Krauss, M., et al., *Occurrence and removal of N-nitrosamines in wastewater treatment plants.* Water Research, 2009. **43**(17): p. 4381-4391.

23. Mirvish, S.S., *Formation of N-nitroso compounds-Chemistry, kinetics, and in vivo occurrence.* Toxicology and Applied Pharmacology, 1975. **31**(3): p. 325-351.

24. Keefer, L.K. and P.P. Roller, *N-nitrozation by nitrite ion in neutral and basic medium.* Science, 1973. **181**(4106): p. 1245-1247.

25. Ohta, T., et al., *Photochemical nitrosation of dimethylamine in aqueous-solution containing nitrite.* Chemosphere, 1982. **11**(8): p. 797-801.

26. Lunn, G., E.B. Sansone, and A.W. Andrews, *Aerial oxidation of hydrazines to nitrosamines.* Environmental and Molecular Mutagenesis, 1991. **17**(1): p. 59-62.

27. Choi, J.H. and R.L. Valentine, *Formation of N-nitrosodimethylamine (NDMA) from reaction of monochloramine: a new disinfection by-product.* Water Research, 2002. **36**(4): p. 817-824.

28. Kimoto, W.I., et al., *Nitrosamines in tap water after concentration by a carbonaceous adsorbent.* Water Research, 1981. **15**(9): p. 1099-1106.

29. Choi, J.H. and R.L. Valentine, *N-nitrosodimethylamine formation hy free-chlorine-enhanced nitrosation of dimethylamine.* Environmental Science & Technology, 2003. **37**(21): p. 4871-4876.

30. Trofe, T.W., G.W. Inman, and J.D. Johnson, *Kinetics of monochloramine decomposition in the presence of bromide.* Environmental Science & Technology, 1980. **14**(5): p. 544-549.

31. Zhao, Y.Y., et al., *Formation of N-nitrosamines from eleven disinfection treatments of seven different surface waters.* Environmental Science & Technology, 2008. **42**(13): p. 4857-4862.

32.   Wilczak, A., et al., *Formation of NDMA in chloraminated water coagulated with DADMAC cationic polymer.* American Water Works Association Journal, 2003. **95**(9): p. 94-106.

33.   Mitch, W.A., A.C. Gerecke, and D.L. Sedlak, *A N-nitrosodimethylamine (NDMA) precursor analysis for chlorination of water and wastewater.* Water Research, 2003. **37**(15): p. 3733-3741.

34.   Druckrey, H., et al., *Organotropism and carcinogenic effects of 65 different N-nitroso compounds in BD-rats* Z krebsforsch, 1967. **69**(2): p. 103-201.

35.   Terracini, B., P.N. Magee, and J.M. Barnes, *Hepatic pathology in rats on low dietary levels of dimethylnitrosamine.* British Journal of Cancer, 1967. **21**(3): p. 559-&.

36.   USEPA, *Record of decision for the western groundwater operable unit OU-3, aerojet Sacramento site.* 2001.

37.   Bellona, C., et al., *Factors affecting the rejection of organic solutes during NF/RO treatment - a literature review.* Water Research, 2004. **38**(12): p. 2795-2809.

38.   Steinle-Darling, E., et al., *Evaluating the impacts of membrane type, coating, fouling, chemical properties and water chemistry on reverse osmosis rejection of seven nitrosoalklyamines, including NDMA.* Water Research, 2007. **41**(17): p. 3959-3967.

39.   von Gunten, U., *Ozonation of drinking water: Part I. Oxidation kinetics and product formation.* Water Research, 2003. **37**(7): p. 1443-1467.

40.   Lee, C., J. Yoon, and U. Von Gunten, *Oxidative degradation of N-nitrosodimethylamine by conventional ozonation and the advanced oxidation process ozone/hydrogen peroxide.* Water Research, 2007. **41**(3): p. 581-590.

41.   Vongunten, U. and J. Holgne, *Bromate formation during ozonation of bromide-containing waters- interaction of ozone and hydroxyl radical reactions.* Environmental Science & Technology, 1994. **28**(7): p. 1234-1242.

42.   Weinberg, H.S., C.A. Delcomyn, and V. Unnam, *Bromate in chlorinated drinking waters: Occurrence and implications for future requlation.* Environmental Science & Technology, 2003. **37**(14): p. 3104-3110.

43.   Lee, C., et al., *UV photolytic mechanism of N-nitrosodimethylamine in water: Dual pathways to methylamine versus dimethylamine.* Environmental Science & Technology, 2005. **39**(7): p. 2101-2106.

44.   Chen, B., et al., *Solar photolysis kinetics of disinfection byproducts.* Water Research, 2010. **44**(11): p. 3401-3409.

45.   Chen, B., P. Westerhoff, and S.W. Krasner, *Fate and transport of wastewater-derived disinfection by-products in surface waters*, in *Disinfection*

By-Products in Drinking Water: Occurrence, Formation, Health Effects, and Control, T. Karanfil, S.W. Krasner, and Y. Xie, Editors. 2008, Amer Chemical Soc. p. 257-273.

46. Plumlee, M.H., et al., *N-nitrosodimethylamine (NDMA) removal by reverse osmosis and UV treatment and analysis via LC-MS/MS.* Water Research, 2008. **42**(1-2): p. 347-355.

47. Zhou, Q.L., et al., *Field evidence of biodegradation of N-Nitrosodimethylamine (NDMA) in groundwater with incidental and active recycled water recharge.* Water Research, 2009. **43**(3): p. 793-805.

48. Sedlak, D.L., et al., *Sources and fate of nitrosodimethylamine and its precursors in municipal wastewater treatment plants.* Water Environment Research, 2005. **77**(1): p. 32-39.

49. Padhye, L., et al., *Occurrence and Fate of Nitrosamines and Their Precursors in Municipal Sludge and Anaerobic Digestion Systems.* Environmental Science & Technology, 2009. **43**(9): p. 3087-3093.

50. Yamazaki, H., et al., *Participation of rat liver cytochrome P450 2E1 in the activation of N-nitrosodimethylamine and N-nitrosodiethylamine to products genotoxic in an acetyltransferase-overexpressing Salmonella typhimurium strain (NM2009).* Carcinogenesis, 1992. **13**(6): p. 979-85.

51. Arciero, D., et al., *Degradation of trichloroethylene by the ammonia-oxidizing bacterium nitrosomonas-eupopaea.* Biochemical and Biophysical Research Communications, 1989. **159**(2): p. 640-643.

52. Smith, C.A., K.T. O'Reilly, and M.R. Hyman, *Characterization of the initial reactions during the cometabolic oxidation of methyl tert-butyl ether by propane-grown Mycobacterium vaccae JOB5.* Applied and Environmental Microbiology, 2003. **69**(2): p. 796-804.

53. Sharp, J.O., T.K. Wood, and L. Alvarez-Cohen, *Aerobic Biodegradation of N-Nitrosodimethylamine (NDMA) by Axenic Bacterial Strains.* Biotechnology and bioengineering, 2005. **89**: p. 11.

54. Sharp, J.O., et al., *An inducible propane monooxygenase is responsible for N-nitrosodimethylamine degradation by Rhodococcus sp. strain RHA1.* Appl Environ Microbiol, 2007. **73**(21): p. 6930-8.

55. Fournier, D., et al., *Biotransformation of N-nitrosodimethylamine by Pseudomonas mendocina KR1.* Appl Environ Microbiol, 2006. **72**(10): p. 6693-8.

56. Fournier, D., et al., *Aerobic biodegradation of N-nitrosodimethylamine by the propanotroph Rhodococcus ruber ENV425.* Appl Environ Microbiol, 2009. **75**(15): p. 5088-93.

57. Heur, Y.H., et al., *The fenton degradation as a nonenzymatic model for microsomal denitrosation of N-nitrosodimethylamine.* Chemical Research in Toxicology, 1989. **2**(4): p. 247-253.

58. Keefer, L.K., et al., *Concurrent generation of methylamine and nitrite during denitrosation of N-nitrosodimethylamine by rat-liver microsomes.* Cancer Research, 1987. **47**(2): p. 447-452.

59. Mallik, M.A.B. and K. Tesfai, *Transformation of nitrosamines in soil and in vitro by soil-microorganisms.* Bulletin of Environmental Contamination and Toxicology, 1981. **27**(1): p. 115-121.

60. Oliver, J.E., P.C. Kearney, and A. Kontson, *Degradation of herbicide-related nitrosamines in aerobic soils.* Journal of Agricultural and Food Chemistry, 1979. **27**(4): p. 887-891.

61. Drewes, J.E., C. Hoppe, and T. Jennings, *Fate and transport of N-nitrosamines under conditions simulating full-scale groundwater recharge operations.* Water Environment Research, 2006. **78**(13): p. 2466-2473.

62. Nalinakumari, B., W. Cha, and P. Fox, *Effects of Primary Substrate Concentration on NDMA Transport during Simulated Aquifer Recharge.* Journal of Environmental Engineering-Asce, 2010. **136**(4): p. 363-370.

63. Yang, W.C., et al., *Degradation of N-nitrosodimethylamine (NDMA) in landscape soils.* Journal of Environmental Quality, 2005. **34**(1): p. 336-341.

64. Zengler, K., *Accessing uncultivated microorganisms: from the environmental to organisms and genomes and back* 2008.

65. Tiedje, J.M., et al., *Opening the black box of soil microbial diversity.* Applied Soil Ecology, 1999. **13**(2): p. 109-122.

66. Edel-Hermann, W., et al., *Terminal restriction fragment length polymorphism analysis of ribosomal RNA genes to assess changes in fungal community structure in soils.* Fems Microbiology Ecology, 2004. **47**(3): p. 397-404.

67. Blackwood, C.B. and J.S. Buyer, *Evaluating the physical capture method of terminal restriction fragment length polymorphism for comparison of soil microbial communities.* Soil Biology & Biochemistry, 2007. **39**(2): p. 590-599.

68. Thies, J.E., *Soil microbial community analysis using terminal restriction fragment length polymorphisms.* Soil Science Society of America Journal, 2007. **71**(2): p. 579-591.

69. Nocker, A., M. Burr, and A.K. Camper, *Genotypic microbial community profiling: A critical technical review.* Microbial Ecology, 2007. **54**(2): p. 276-289.

70. Liu, W.T., et al., *Characterization of microbial diversity by determining terminal restriction fragment length polymorphisms of genes encoding 16S rRNA.*

Applied and Environmental Microbiology, 1997. **63**(11): p. 4516-4522.

71. Zengler, K., et al., *Cultivating the uncultured.* Proceedings of the National Academy of Sciences of the United States of America. 2002.

72. Osborn, A.M., E.R.B. Moore, and K.N. Timmis, *An evaluation of terminal-restriction fragment length polymorphism (T-RFLP) analysis for the study of microbial community structure and dynamics.* Environmental Microbiology, 2000. **2**(1): p. 39-50.

73. Fedi, S., et al., *T-RFLP analysis of bacterial communities in cyclodextrin-amended bioreactors developed for biodegradation of polychlorinated biphenyls.* Research in Microbiology, 2005. **156**(2): p. 201-210.

74. Dickie, I.A., B. Xu, and R.T. Koide, *Vertical niche differentiation of ectomycorrhizal hyphae in soil as shown by T-RFLP analysis.* New Phytologist, 2002. **156**(3): p. 527-535.

75. Katsivela, E., et al., *Bacterial community dynamics during in-situ bioremediation of petroleum waste sludge in landfarming sites.* Biodegradation, 2005. **16**(2): p. 169-180.

76. Marsh, T.L., et al., *Terminal restriction fragment length polymorphism analysis program, a web-based research tool for microbial community analysis.* Applied and Environmental Microbiology, 2000. **66**(8): p. 3616-3620.

77. Kent, A.D., et al., *Web-based phylogenetic assignment tool for analysis of terminal restriction fragment length polymorphism profiles of microbial communities.* Applied and Environmental Microbiology, 2003. **69**(11): p. 6768-6776.

78. Sambrook, J. and D.W. Russell, *The condensed protocols from Molecular cloning : a laboratory manual.* 2006, Cold Spring Harbor, N.Y.: Cold Spring Harbor Laboratory Press.

79. Gurtler, V., V.A. Wilson, and B.C. Mayall, *Classification of medically important clostridia using restriction endonuclease site differences of PCR-amplified 16S rDNA.* J Gen Microbiol, 1991. **137**(11): p. 2673-9.

80. Felske, A., et al., *Ribosome analysis reveals prominent activity of an uncultured member of the class Actinobacteria in grassland soils.* Microbiology-Uk, 1997. **143**: p. 2983-2989.

81. Lane, D.J., et al., *Rapid-determination of 16S ribosomal-RNA sequences for phylogenetic analyses.* Proceedings of the National Academy of Sciences of the United States of America, 1985. **82**(20): p. 6955-6959.

82. Gurtler, V., *Typing of clostridium-difficile strains by PCR-amplification of variable-length 16S-23S rDNA spacer regions.* Journal of General Microbiology, 1993. **139**: p. 3089-3097.

83. Watanabe, K., Y. Kodama, and S. Harayama, *Design and evaluation of PCR primers to amplify bacterial 16S ribosomal DNA fragments used for community fingerprinting.* Journal of Microbiological Methods, 2001. **44**(3): p. 253-262.

84. Madigan, M.T. and J.M. Martinko, *Brock Biology of Microorganisms* 11th ed. 2007.

85. *Standard Methods for the Examination of Water and Wastewater.* 20 ed. 1998: American Public Health Association.

86. Wang, H.F., H.K. Chang, and H.W. Chao, *Determination of the total nitrogen in waste water with 2, 6-dimethylphenol by spectrophotometry.* Chemical analysis and measurement, 2003. **12**(6): p. 20-21.

87. Stolz, A., *Molecular characteristics of xenobiotic-degrading sphingomonads.* Applied Microbiology and Biotechnology, 2009. **81**(5): p. 793-811.

88. Toyama, T., et al., *Biodegradation of bisphenol A and bisphenol F in the rhizosphere sediment of Phragmites australis.* Journal of Bioscience and Bioengineering, 2009. **108**(2): p. 147-150.

89. Ushiba, Y., Y. Takahara, and H. Ohta, *Sphingobium amiense sp nov., a novel nonylphenol-degrading bacterium isolated from a river sediment.* International Journal of Systematic and Evolutionary Microbiology, 2003. **53**: p. 2045-2048.

90. Liang, Q.F. and G. Lloyd-Jones, *Sphingobium scionense sp nov., an aromatic hydrocarbon-degrading bacterium isolated from contaminated sawmill soil.* International Journal of Systematic and Evolutionary Microbiology, 2010. **60**: p. 413-416.

91. Collins, M.D., M. Dorsch, and E. Stackebrandt, *Transfer of Pimelobacter-tumescens to Terrabacter gen-nov as terrabacter-tumescens comb nov and of Pimelobacter-jensenii to Nocardioides as Nocardioides-jensenii comb nov.* International Journal of Systematic Bacteriology, 1989. **39**(1): p. 1-6.

92. Lee, J.E., et al., *Terrabacter lapilli sp nov., an actinomycete isolated from stone.* International Journal of Systematic and Evolutionary Microbiology, 2008. **58**: p. 1084-1088.

93. Weon, H.Y., et al., *Terrabacter aeriphilus sp nov., isolated from an air sample.* International Journal of Systematic and Evolutionary Microbiology, 2010. **60**: p. 1130-1134.

94. Yoon, J.H., et al., *Terrabacter terrigena sp nov., isolated from soil.* International Journal of Systematic and Evolutionary Microbiology, 2009. **59**: p. 2798-2802.

95. Green, P.N., *Methylobacterium.* Prokaryotes: A Handbook on the Biology of Bacteria, Vol 5, Third Edition:PROTEOBACTERIA: ALPHA AND BETA SUBCLASSES, ed. M. Dworkin, et al. 2006: Springer. 257-265.

96. Poonguzhali, S., M. Madhaiyan, and T. Sa, *Production of acyl-homoserine*

lactone quorum-sensing signals is widespread in gram-negative *Methylobacterium.* Journal of Microbiology and Biotechnology, 2007. **17**(2): p. 226-233.

97. Wang, X., et al., *Methylobacterium salsuginis sp. nov., isolated from seawater.* Int J Syst Evol Microbiol, 2007. **57**(Pt 8): p. 1699-703.

98. Lee, S.W., et al., *Methylobacterium dankookense sp nov., isolated from drinking water.* Journal of Microbiology, 2009. **47**(6): p. 716-720.

99. Hiraishi, A., et al., *Phenotypic and genetic diversity of chlorine-resistant Methylobacterium strains isolated from various environments.* Appl Environ Microbiol, 1995. **61**(6): p. 2099-107.

100. Drobniewski, F.A., *Bacillus Cereus and related species.* Clinical Microbiology Reviews, 1993. **6**(4): p. 324-338.

101. Agata, N., M. Ohta, and K. Yokoyama, *Production of Bacillus cereus emetic toxin (cereulide) in various foods.* International Journal of Food Microbiology, 2002. **73**(1): p. 23-27.

102. Cronin, U.P. and M.G. Wilkinson, *The potential of flow cytometry in the study of Bacillus cereus.* Journal of Applied Microbiology, 2010. **108**(1): p. 1-16.

103. Bala, K., P. Sharma, and R. Lal, *Sphingobium quisquiliarum sp nov., a hexachlorocyclohexane (HCH)-degrading bacterium isolated from an HCH-contaminated soil.* International Journal of Systematic and Evolutionary Microbiology, 2010. **60**: p. 429-433.

104. Young, C.C., et al., *Sphingobium olei sp nov., isolated from oil-contaminated soil.* International Journal of Systematic and Evolutionary Microbiology, 2007. **57**: p. 2613-2617.

105. Doronina, N.V., et al., *Methylobacterium suomiense sp nov and Methylobacterium lusitanum sp nov., aerobic, pink-pigmented, facultatively methylotrophic bacteria.* International Journal of Systematic and Evolutionary Microbiology, 2002. **52**: p. 773-776.

106. Campbell, N.A. and J.B. Reece, *Biology.* 6th ed.

107. Bisswanger, H., *Enzyme kinetics. Principles and methods.* 1st ed. 2002.

108. Blackwood, C.B., et al., *Terminal restriction fragment length polymorphism data analysis for quantitative comparison of microbial communities.* Applied and Environmental Microbiology, 2003. **69**(2): p. 926-932.

Appendixes

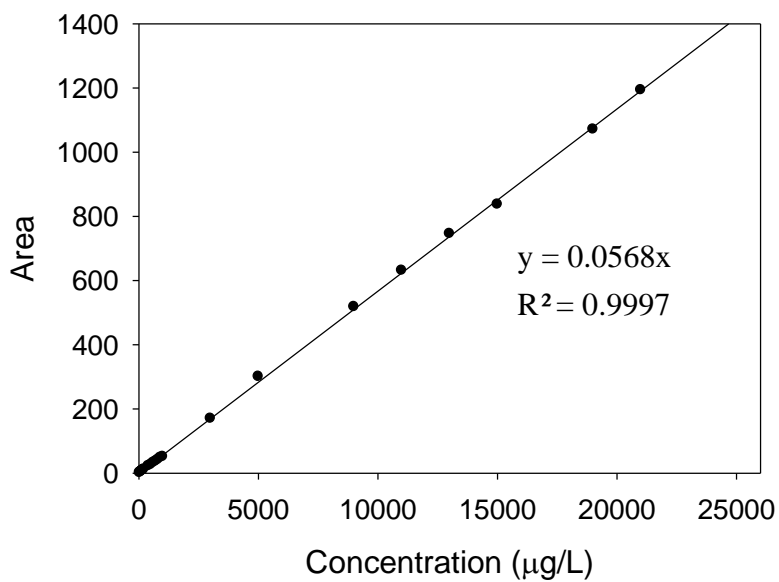$y = 0.0568x$

$R^2 = 0.9997$

Figure A. 1   Calibration curve of NDMA
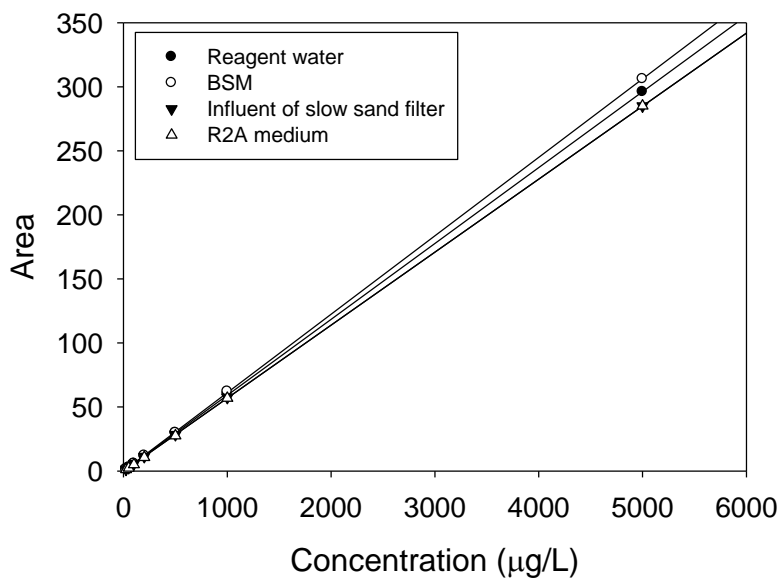

Figure A. 2   Calibration curves of NDMA in different matrixes
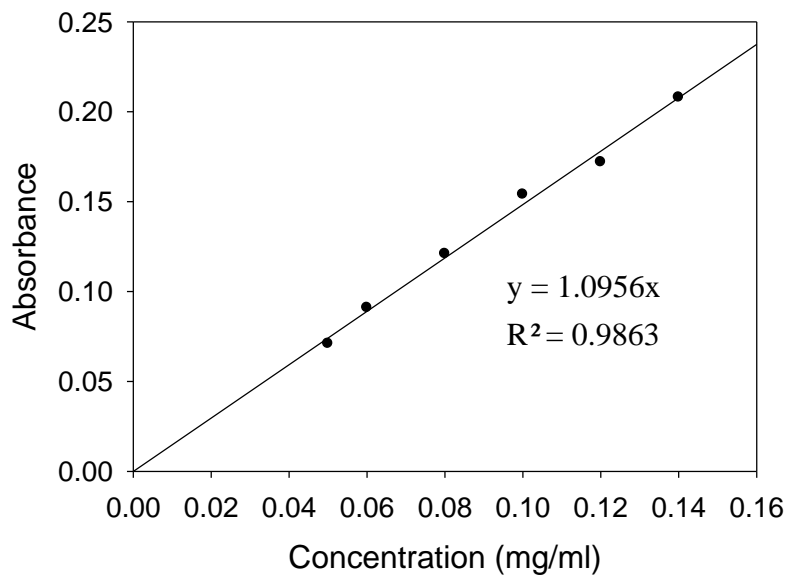
I

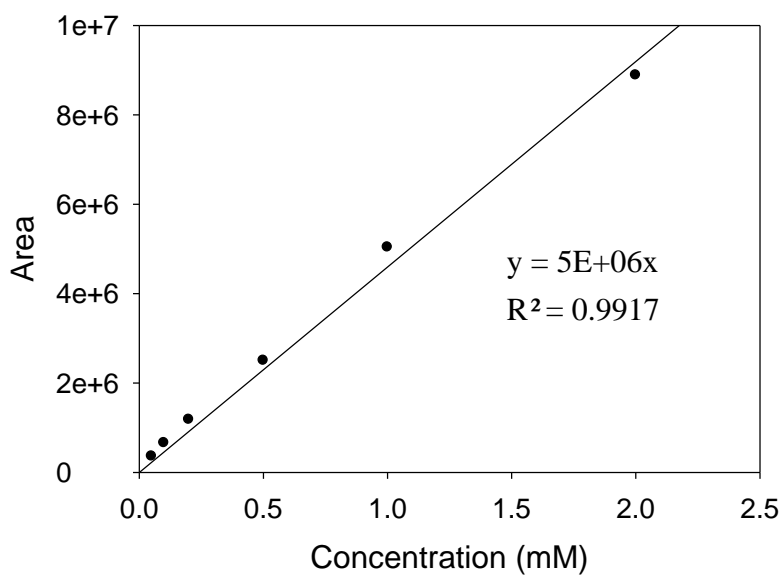Figure A. 3   Calibration curves of protein density

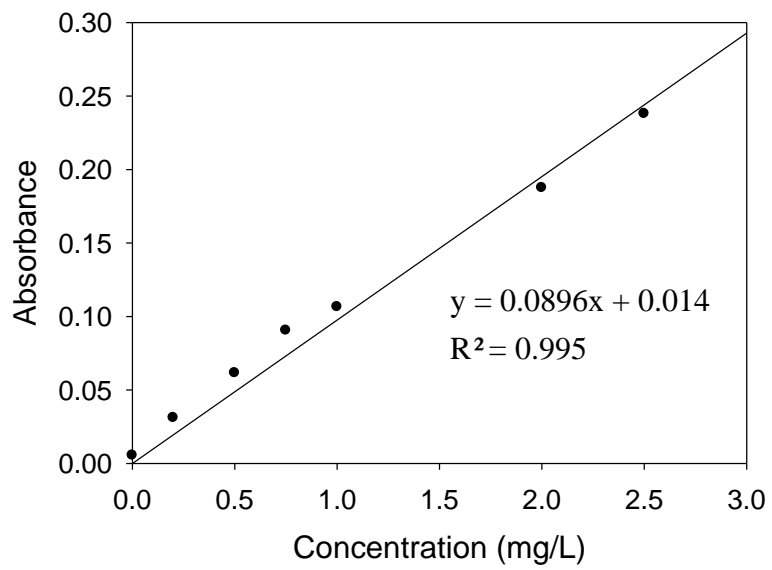Figure A. 4   Calibration curve of methanol

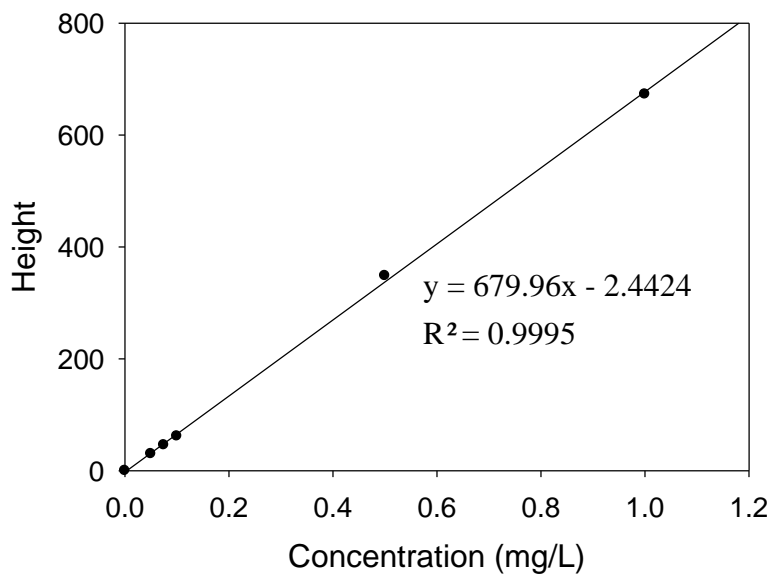Figure A. 5　　Calibration curve of total dissolved nitrogen (TDN)

$y = 0.0896x + 0.014$
$R^2 = 0.995$

Figure A. 6　　Calibration curve of nitrate (NO_3^-)
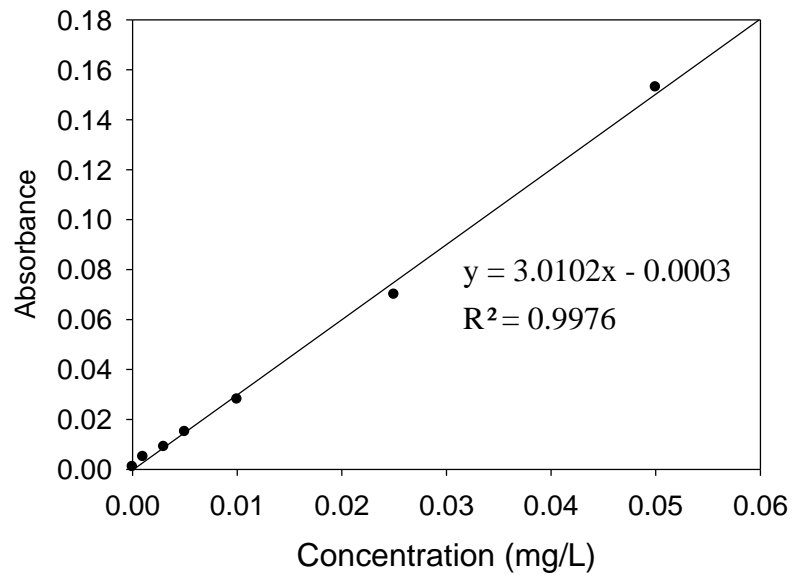
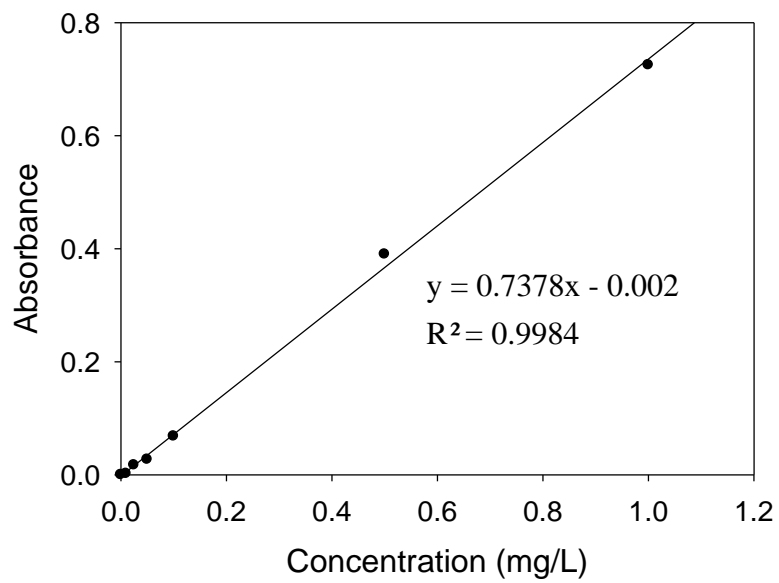$y = 679.96x - 2.4424$
$R^2 = 0.9995$

Figure A. 7   Calibration curve of nitrite (NO_2^-)

Figure A. 8   Calibration curve of ammonium (NH_4^+)